

$U(1)$ Fields from Qubits: an Approach via D-theory Algebra

David Berenstein[†], Richard Brower[‡], and Hiroki Kawai[†]

[†]Department of Physics, University of California at Santa Barbara,
CA 93106

[‡]Department of Physics, Boston University, Boston, MA 02215

January 10, 2022

Abstract

A new quantum link [1, 2] microstructure was proposed for the lattice QCD Hamiltonian, replacing the Wilson gauge links by a bilinear of fermionic qubits, later generalized to D-theory [3]. This formalism provides a general framework for building lattice field theory algorithms for quantum computing [4]. We focus mostly on the simplest case of a quantum rotor for a single compact $U(1)$ field. We also make some progress for non-abelian setups, making it clear that the ideas developed in the $U(1)$ case extend to other groups. These in turn are building blocks for $1+0$ matrix models, $1+1$ sigma models and non-Abelian gauge theories in $2+1$ and $3+1$ dimensions. By introducing multiple flavors [5, 6] for the $U(1)$ field, where the flavor symmetry is gauged, we can efficiently approach the infinite-dimensional Hilbert space of the quantum $O(2)$ rotor with increasing flavors. The emphasis of the method is on preserving the symplectic algebra exchanging fermionic qubits by sigma matrices (or hard bosons) and developing a formal strategy capable of generalization to $SU(3)$ field for lattice QCD and other non-Abelian $1+1$ sigma models or $1+3$ gauge theories. For $U(1)$ we discuss briefly the qubit algorithms for the study of the discrete $1+1$ Sine-Gordon equation.

Contents

1	Introduction	2
2	Symplectic Algebra and Universality	5
2.1	Fermionic D-Theory Algebra	6
2.2	Non-Abelian Generalizations	10
3	Target $U(1)$ Quantum Rotor	14
4	Complexity of qubit Realizations	17
4.1	Phase space considerations.	20
4.2	Exponential Formats	22
4.3	Linear Formats and Sparsity	24
5	Spectral Matching of D-theory Truncation	26
6	Applications to $1 + 1$ Field Theories.	31
6.1	Real-time evolution	32
6.2	Gapped/gapless phase transition	33
7	Discussion	36

1 Introduction

Lattice field theory, particularly the Wilson formulation of Quantum Chromodynamics [7], now plays a central role in High Energy Physics capable of *ab initio* precise predictions in support of the search for physics beyond the standard model (BMS). This is due to a firm theoretical foundation, combined with spectacular advances in algorithms on classical computers soon to approach the Exascale. It is generally accepted that Wilson Euclidean (imaginary time) lattice action lies in the basin of attraction of QCD, converging to the exact answer in infinite volume (IR) and zero lattice spacing (UV) limits.

However, the standard Monte Carlo integration is incapable of real-time dynamics. Quantum computing could change this paradigm. This requires not only the development of quantum computing technology but as first noted by Feynman in 1982, the transformation of lattice field theories to an appropriate Hamiltonian \hat{H} expressed in terms of qubits (sigma matrix operation). The first step to convert the Wilson action to a Hamiltonian formulation is straight forward. For example, for QCD by taking the time continuum limit of the transfer matrix in the Wilson's lattice QCD, one obtains the Kogut-Suskind Hamiltonian operator

$$\hat{H}_{QCD} = \frac{g^2}{2} \sum_{\langle x,y \rangle} Tr[E^2(x,y)] + \frac{1}{g^2} \sum_{x,\mu \neq \nu} Tr[2 - U_{\mu\nu}(x) - U_{\mu\nu}^\dagger(x)] + \Psi^\dagger D[U] \Psi. \quad (1)$$

The electric fields operators ¹, $E(x,y)$, are conjugate to the gauge fields, $A(x,y)$, that determine the Wilson links $U(x,y) = \exp[iA(x,y)]$ in the gauge group. The quark term is $\Psi^\dagger D[U] \Psi$. The symplectic algebra on each link $\langle x,y \rangle$ between $E(x,y)$ and $U(x,y)$ preserves the exact spatial gauge invariance and the Gauss' law. It is then anticipated, based on the Osterwalder-Schrader positivity, that the unitary evolution operator $U(t,0) = \exp[-it\hat{H}_{QCD}]$ of the lattice Hilbert space, also converges to the exact quantum dynamics as the UV lattice spacing and finite volume IR cutoff are removed.

The second step, converting the problem into qubits, at least on all proposed hard-

¹On a regular hypercubic lattice, fields on directed links $\langle x,y \rangle$ with a positive shift, $y = x + \mu$ are often labelled by $U_\mu(x) = U(x, x + \mu)$ and the somewhat awkward backward link by $U_\mu^\dagger(x - \mu) = U(x + \mu, x)$. The discrete curl for the magnetic term is then the path ordered product on each square: $U_{\mu\nu}(x) = U(x, x + \mu)U(x + \mu, x + \nu)U(x + \nu, x + \mu)U(x + \nu, x)$.

ware, is more difficult. The local variables at a single link, when quantized, produce an infinite-dimensional Hilbert space. This is $L^2(G)$ for G the local gauge group. Roughly speaking, we have a wave function of the classical group variable g , $\psi(g)$, which needs to be normalizable. For example for QCD, the infinite-dimensional Hilbert space of the $SU(3)$ group manifold at each link must be drastically reduced. On modern classical computers, this is solved by the illusion of the continuum with a mild 32 or 64-bit truncation of floating arithmetic approximation, but at present on proposed quantum hardware that has a limited number of qubits, this Hilbert space must be represented by a small number of qubits per lattice site. The problem is to invent a new microstructure for a qubit Hamiltonian operator that falls into the **universality class** of the Kogut-Suskind Hamiltonian. At least in that sense, when we take the large volume, small lattice size limit, we should recover QCD for the low energy states near the vacuum.

A general framework, referred as Quantum Links[1, 2, 3] or more properly, its generalization called D-theory [8] has been proposed to achieve this. In D-theory, \hat{E} and \hat{U} operators on each link are represented by the bilinears of a small set of Fermionic qubits. This is an explicit example of what Bravyi and Kitaev [9] refer to as local fermionic modes (LFM). The basic heuristic to plausibly reach the correct universality class is to attempt to choose wisely the base lattice to satisfy a maximal set of space symmetries and as well to find field operators which still satisfies the basic symplectic algebra of the Kogut-Suskind Hamiltonian ². The latter field Hilbert space is our focus, emphasizing the simplest $U(1)$ group manifold. It is plausible that, by preserving lattice symmetries and the symplectic structure, simple examples can be found in the basin of attraction of continuum field theory as indeed first conjectured by Richard Feynman [10] in 1982.

Of course, to establish that a Hamiltonian is in a universality class is a difficult problem, generally requiring both theoretical insight and numerical evidence. The original D-theory paper argued that for asymptotically free chiral models in $1 + 1$ dimensions and gauge theories in $1 + 3$ dimensions, universality would be valid with only a logarithmic growing layering of a single qubit in an extra dimension [5]. While this is a modest increase in the volume, the discovery of other options is anticipated as illustrated by the evidence found [11], of a lattice Hamiltonian for $1 + 1$ -D non-linear $O(3)$ sigma model with two layers. The qubit systems exhibit both the UV asymptotic

²Here we mean that we preserve exactly the local symmetry of gauge transformations on the local link variables

free fixed point and the IR universality in the continuum. For our $U(1)$ example, the reader is also referred to the study by Zhang, Meurice and Tsai [12], where in the presence of truncation effects, it is noticed that the Berezinskii-Kosterlitz-Thouless (BKT) transition for quantum links is absent for 3 states but appears for 5 states per site or more. The lesson here is that if the truncation is too drastic one might be outside the correct Universality class.

Here we consider the limited question of how the use of M copies of fermionic qubits (referred to as a flavor index in Ref.[5, 6]) at each link can converge locally to the Kogut-Suskind Hamiltonian as $M \rightarrow \infty$. This sequence provides a qubit implementation that can be explored with respect to universality and efficient quantum computing with the hope that very few qubits per lattice volume suffice. This paper is also restricted to the simplest example: a compact $U(1)$ field manifold formulated in a way that is capable of generalization to non-Abelian group manifolds. Even in this Abelian example, the Lagrangian formalism is mapped to a non-trivial $SU(2)$ quantum rotor as a Hamiltonian, a basic ingredient of many qubit codes and even their hardware realization [13, 14]. Applications are interesting for a variety of quantum fields theories, not just gauge theories. Depending on if we have certain gauge constraints or not, the fact that the fields give an interesting local Hilbert space structure at a site or link is what matters. The main analysis of local fields can be applied to examples such as the XY model, the Sine-Gordon theory or the Schwinger model in $1 + 1$ dimensions and gauge theories in $d = 3$ and $d = 4$ dimensions. For example, in the discretized version of the Sine-Gordon model, the local variable can also be taken to be a periodic variable living on the sites of the lattice rather than the links. We would also have $L^2(S^1)$ as the quantization of the local variable, much like the $U(1)$ theory we study. A similar comment would be applied to non-linear sigma models on group manifolds where we would obtain $L^2(G)$ at each site, rather than $L^2(G)$ on links with the additional Gauss' law constraints (local gauge invariance). In this sense, this paper is more concerned with the individual manifold for fields that can be put on a link or lattice site, rather than the problem of a full quantum theory. We are basically asking how to generate local variables that become bosons (with a non-trivial manifold and symmetry structure) when the cutoff on the local variable is removed, while the symmetry structure is realized exactly.

The paper is organized as follows. In Sec. 2, we present the general algebraic constraint of quantum links for the $U(N)$ field with multiple flavors which is specialized to $U(1)$, and we also comment on how the quantum links with gauged flavor give a description that is a truncation of the Hilbert space of more general group manifolds

with no additional states. In Sec. 3, we define the truncation of the $U(1)$ quantum Hamiltonian both for the D-theory flux cutoff and the Z_N clock rotor fields truncation. In Sec. 4 we implement the quantum fermionic qubits for the sigma matrices without the use of Wigner Jordan transformations. In Sec. 5, we numerically compare the spectra of the finitized models in our formalism as well as that of the Z_N clock rotor fields truncation. Sec. 6 consider briefly the quantum circuits to implement the $1 + 1$ -D XY and Sine-Gordon models for the lowest triplet truncation. In Sec. 7, we elaborate further on our results.

2 Symplectic Algebra and Universality

A quantum Hamiltonian, just like its classical counterpart is defined by the symplectic structure of its P - Q coordinates expressed as canonical commutators, or as the Poisson brackets respectively. Using the the Kogut-Susskind Hamiltonian as an example to motivate the D-theory construction, we first double the phase space introducing a left right pair, $E_L(x, y)$, $\hat{E}_R(x, y)$ electric fields or gauge generators on each link and a pair of forward and backward link operators $U(x, y)$ and $U(y, x) = U^\dagger(x, y)$.

$$\hat{H} = \frac{g^2}{4} \sum_{\langle x, y \rangle} \text{Tr}[E_L^2(x, y) + E_R^2(x, y)] + \frac{1}{g^2} \sum_{x, \mu \neq \nu} \text{Tr}[2 - U_{\mu, \nu}(x) - U_{\mu, \nu}^\dagger(x)] \quad (2)$$

At first, it might seem strange that one has to double the variables. This is quite natural when studying motion on a group manifold. This is because we have two possible group actions on G , by the left and right multiplication. There are generators of both of these transformations, which will end up being the electric fields (the canonical conjugates to the group variables).

It is also known that it is convenient to study the left and right invariant forms, $U^{-1}dU$ and dUU^{-1} , which lead to velocities $v_L = U^{-1}\dot{U}$ and $v_R = \dot{U}U^{-1}$. Each of these can serve as a basis for velocities, and they are clearly related to each other by

$$v_R = Uv_LU^{-1}. \quad (3)$$

When one is careful with these velocities, we get canonical conjugates to the group variables that encode the symmetry. These are Lie algebra valued, generating group

transformations in the Hamiltonian sense, and the left and right actions on G commute with each other.

The original Hamiltonian is then recovered with the constraint of unitarity and the constraint inherited from the velocities Eq. (3) on each link $\langle xy \rangle$

$$U^\dagger(x, y)U(x, y) = 1 \quad , \quad E_R(x, y) = U(x, y)E_L(x, y)U^\dagger(x, y) \quad (4)$$

A fermionic matter term $\hat{H}_\psi = \Psi^\dagger D[U]\Psi$, is straight forward to add, but not essential for our current discussion.

The full symplectic algebra on each link $\langle x, y \rangle$ in the doubled phase space is summarized as

$$[E_L^\alpha, U] = \lambda_\alpha U \quad , \quad [E_R^\alpha, U] = -U\lambda_\alpha \quad , \quad [E_L^\alpha, U^\dagger] = -U^\dagger\lambda_\alpha \quad , \quad [E_R^\alpha, U^\dagger] = \lambda_\alpha U^\dagger \quad (5)$$

with two independent Lie algebras

$$[E_L^\alpha, E_L^\beta] = if_\gamma^{\alpha\beta} E_L^\gamma \quad , \quad [E_R^\alpha, E_R^\beta] = if_\gamma^{\alpha\beta} E_R^\gamma \quad , \quad [E_L^\alpha, E_R^\beta] = 0 \quad (6)$$

for the operators, $E_{L/R}^{ij} = \lambda_\alpha^{ij} E_{L/R}^\alpha$. Basically, on the left action of E_L , U is like the fundamental, whereas on the right action E_R it is like the anti-fundamental. The roles are reversed for U^\dagger which transforms oppositely to U . The U variables, which play the role of position variables, of both U and U^\dagger commute with each other (their matrix elements commute).

Preserving the symplectic structure would mean that we keep either Eq. (5) and Eq. (6), or we keep Eq. (4). If we keep both, we keep the full $L^2(G)$ which is infinite-dimensional.

2.1 Fermionic D-Theory Algebra

A straight forward discrete representation that exactly preserves the symplectic algebra in Eqs. (5)-(6) replaces the compact field, for example, $U(N)$, by a bilinear of lattice fermions,

$$U_j^i \rightarrow \hat{U}_j^i = \vec{a}^i \cdot \vec{b}_j^\dagger = \sum_m (a^{\dagger m} b_m)_j^i \quad , \quad (U^\dagger)_i^j \rightarrow (\hat{U}^\dagger)_i^j = \vec{b}^j \cdot \vec{a}_i^\dagger = \sum_m (b^{\dagger m} a_m)_i^j \quad (7)$$

The scalar product implies a sum over the vector of M flavors of creation and destruction operators: $\vec{a}^i = (a_1^i, a_2^i \cdots a_M^i)$, $\vec{b}^j = (b_1^j, b_2^j, \cdots, b_M^j)$. All the fermionic operator across the lattice including the $4N_c M$ operators $(a_m^i(x, y), b_m^i(x, y))$ per link obey the standard anti-commutator relations of single fermionic degrees of freedom, as introduced in [5, 6]. The symplectic algebra fixes the electric flux representation,

$$\hat{E}_{L,j}^i = (\vec{a}^\dagger \cdot \vec{a})_j^i = \sum_m (a_m^\dagger a_m)_j^i \quad , \quad \hat{E}_{R,j}^i = (\vec{b}^\dagger \cdot \vec{b})_j^i = \sum_m (b_m^\dagger b_m)_j^i \quad (8)$$

to reproduce the exact gauge algebra in Eq. (6). Although this seems cumbersome, the a operators carry the left action and the b operators carry the right action. In this way, E_L, E_R have been separated into completely distinct variables. Each flavor of a carries the same representation with respect to the left Lie algebra: the fundamental. The same is true with b . The flavor index m only appears in sums, so it can be thought of as a $U(M)$ local constraint on each link. It is this constraint that ties the left and the right actions to each other eventually.

The resulting fermionic qubit form, referred in Bravyi and Kitaev [9] as **local fermionic modes**, is a small finite Fock space on each lattice site or link. The original link variables $U(x, y)$ commute with each other, whereas in the fermionic representation, this is not maintained. The only non-zero commutator is local to each link:

$$[\hat{U}_j^i, (\hat{U}^\dagger)_l^k] = \hat{E}_{L,l}^i \delta_j^k - \hat{E}_{R,j}^k \delta_l^i \quad \implies \quad [\hat{U}, \hat{U}^\dagger]_j^i = N(\hat{E}_{L,j}^i - \hat{E}_{R,j}^i) \quad , \quad (9)$$

Thus, a link matrix is no longer normal and as a consequence, also breaks the unitarity $UU^\dagger = 1$. The symplectic algebra at each link treats E_L and E_R as independent *velocity coordinates*, conjugate to non-commuting *positions* operators, \hat{U} and \hat{U}^\dagger .

This breaking should be interpreted in its entirety as an irrelevant UV cutoff effect. As we go to the continuum limit, with sums of multiple paths between distance sources, this non-commutation due to infrequent intersection at the cutoff scale should become vanishing small in the continuum limit. Moreover, when averaging over paths over long distances, we would also abandon the constraint $UU^\dagger = 1$, which is not satisfied when we use expectation values for U and U^\dagger separately.

It should also be noted that this fermionic construction of operators in the multi-flavor Hilbert space satisfying the symplectic algebra is not unique but provides a general framework to implement multiple solutions which can be adapted to better

approximate the infinite Hilbert space with M flavors and provide alternative qubit implementations to optimize quantum codes. Indeed, it is this flexibility of the D-theory framework which we exploit in the current application for $U(1)$. As we will show explicitly for the $U(1)$ example, the multi-flavor fermionic space factorizes into super selection sectors which can be modified to give a sequence of bosonic qubit models restoring the zero commutator in the limit of $M \rightarrow \infty$.

It is important to note that the $4N^2$ bilinears, $\vec{a}^\dagger \cdot \vec{a}$, $\vec{a}^\dagger \cdot \vec{b}$, $\vec{b}^\dagger \cdot \vec{a}$, $\vec{b}^\dagger \cdot \vec{b}$, for $U(N)$ D-theory are generators of the $U(2N)$ Lie algebra:

$$\begin{bmatrix} \hat{E}_L & \hat{U}^\dagger \\ \hat{U} & \hat{E}^R \end{bmatrix}_j^i = \begin{bmatrix} \vec{a}^\dagger \cdot \vec{a} & \vec{a}^\dagger \cdot \vec{b} \\ \vec{b}^\dagger \cdot \vec{a} & \vec{b}^\dagger \cdot \vec{b} \end{bmatrix}_j^i \quad (10)$$

The key consequence for the D-theory (or quantum links for gauge theories) is the exact preservation of the Lie algebra (the local symmetry transformations). Hamiltonian evolution remains in this $U(2N)$ group manifold at each link. The spin theory has global symmetry generators $\hat{J}_L = \sum_x \hat{E}_L(x)$ and $\hat{J}_R = \sum_R \hat{E}_R(x)$ so that $[\hat{J}_L, \hat{H}] = [\hat{J}_R, \hat{H}] = 0$. It is more remarkable for gauge theories that the quantum link Hamiltonian preserves exactly the local symmetry rotation at each site. Whether or not this radical reduction of the degrees of freedom is capable of reaching a universal continuum fixed point is generally a difficult dynamical question. We will not attempt to solve this problem.

Let us consider for the time being the simplest case of $U(1)$. Via this construction with bifermions we get the Lie algebra of $U(2)$ from all the bilinears. The diagonal $U(1)$ will play no role, as it commutes with all the generators and therefore decouples. More precisely, acting with any of the other elements of the algebra will not change the $U(1)$ diagonal charge, so it will act as a c-number when we think of a physical realization. We are left over with a symplectic structure that has the structure of the Lie algebra of $SU(2)$. Is there another way to motivate this? The answer is yes. The idea is that the original problem of the $U(1)$ theory, when thought of as a classical phase space leads to a cylinder: the tangent bundle of the circle. This has an infinite volume, and therefore the Hilbert space is infinite-dimensional. We can ask if there is any other two-dimensional manifold with a finite volume and a $U(1)$ symmetry. The answer is, not surprisingly, yes; the two-sphere satisfies that condition³. The symplectic structure of the topological two-sphere can also be written

³Also the two-torus

in terms of angular momentum commutation relations (they would play the role of x, y, z coordinates, with a constraint $x^2 + y^2 + z^2 = 1$). This would lead us to recover the formulation above in terms of $SU(2)$ without ever mentioning the fermions. Upon quantization, we should get a fixed $SU(2)$ representation: a fixed value of the central element $x^2 + y^2 + z^2$. This phase space is the homogeneous space manifold $SU(2)/U(1) \simeq \mathbb{CP}^1$, which is the complex projective plane of dimension one. To quantize this quotient space we only need to choose the magnetic flux through the sphere (we need to choose a line bundle over the projective manifold to define the allowed wave functions). One can ask how this works for other groups: what is the manifold that needs to be quantized? The structure of coherent states in [5] seems to have the answer: for $U(N)$ it is the complex Grassmannian $\mathbb{G}(N, 2N) \sim U(2N)/U(N) \times U(N)$. This is also a complex geometry of dimension $2N^2$ and thus can be viewed as a phase space. More importantly, it has a group action by $U(N) \times U(N)$ acting on the left, so it is a candidate phase space with the correct group action. At the level of Lie algebras, the Lie algebra of $U(2N)$ provides the equivalent coordinates to x, y, z above. One can assume that this type of Grassmannian structure will be important in all such realizations for different compact groups.

Going back to our main example, to discretize the $U(1)$ phase space physics, we get a quantum rotor. What should be remembered is that the metric of the two-sphere does not mean much as far as the symplectic structure is concerned, and we could just as well have an elongated sphere. That this is so is because we are studying Hamiltonian physics on the sphere and not a sigma model. What matters is how different functions on the geometry generate dynamical flows. When we elongate the sphere further we can produce a cylinder in the limit of infinite elongation (we can approach the infinite volume of the cylinder this way). A classical Hamiltonian function on the center band of the cylinder and the center band of the elongated sphere could be very similar. This is what is usually represented by the kinetic term p_θ^2 , plus any small perturbation in the angular variable (the base coordinate θ). In this case, p_θ^2 is replaced by L_z^2 in the rotor picture. This band is where the low energy physics of the small kinetic term will be concentrated. At least semi-classically, one can argue that if one low energy band of the cylinder leads to the correct universality class of some favored physics, then for a sufficiently elongated sphere (meaning the elongated sphere has a big enough volume to capture this band) one should land in the same universality class.

Going back to the general case, once the qubit operators are defined for the rotor problem (the $SU(2N)$ generators), the construction of the formalism will apply to

any local quantum field both with local gauge transformations relating different links to each other or for example to spin models such as a 1 + 1-D chiral theory

$$\hat{H}_{chiral} = \sum_x \text{Tr}[\hat{E}_L^2(x)] + \text{Tr}[\hat{E}_R^2(x)] + \lambda \sum_{\langle x,y \rangle} \text{Tr}[2 - \hat{U}(x)\hat{U}^\dagger(y) - \hat{U}(y)\hat{U}^\dagger(x)] \quad (11)$$

with global $U(N)$ symmetries. The term with the coupling λ is the square of the discretized difference equation $(U(x) - U(y))^\dagger (U(x) - U(y))$. The spin theory will have global symmetry generators $\hat{J}_L = \sum_x \hat{E}_L(x)$ and $\hat{J}_R = \sum_R \hat{E}_R(x)$ so that $[\hat{J}_L, \hat{H}] = [\hat{J}_R, \hat{H}] = 0$, where all fields transform as $U(x) \rightarrow gU(x)h^{-1}$ for common g, h . We also refer the reader to reference [8] for other group manifolds. For example, the algebraic structure for $SO(N)$, $SU(N)$, and $Sp(N)$ gauge theories naturally lie in $SO(2N)$, $SU(2N)$ and $Sp(2N)$ algebras respectively and as well as $O(N)$, $U(N) \otimes U(N)$ quantum spin models.

As we will note in detail for our $U(1)$ example, this multi-flavor D-theory Hamiltonian is far from a unique solution to the algebra. Instead, it is useful to construct a variety of D-theory candidates to explore our $U(1)$ examples, which will be carried in Sec. 4.

The generalization for multi-flavor convergence to continuum non-Abelian group manifolds is more involved. We briefly outline the method based on a more group theoretical convergence to the continuum Hilbert space covered by the Peter-Weil theorem. Although this illuminates our method, the reader may choose to go directly to the Sec. 3 on the $U(1)$ example. It is possible to show in general that the state space is easily projected into a subspace with each link represented by a few hard boson (or sigma matrix) qubits. This representation is trivial for $U(1)$ and only requires a local Jordan-Wigner transformation inside the group at each link.

2.2 Non-Abelian Generalizations

We want to show that a similar construction for non-abelian theories gives an approximation of the correct Hilbert space $L^2(U(N))$. For the $U(1)$ case, the $SU(2)$ theory gives rise to a single representation of $SU(2)$ and the different charge states are the different eigenvalues of L_z , giving a cutoff on the $U(1)$ charges that can be realized on a single local field variable. For $U(N)$ we want to show that we also get a list of states with the right charges and a cutoff on the representations, with no additional states that would need to be eliminated in the Hamiltonian.

It is convenient for us to consider a slightly modified realization of the U variables as bilinear in the fermions. As described in equation Eq. (7), the operators U and U^\dagger leave a total occupation number unchanged. There is an automorphism of fermion algebras $a_m^j \leftrightarrow c_m^{j\dagger}$ and $a_j^{\dagger m} \leftrightarrow c_j^m$ which makes it possible to describe U as made purely from raising operators and U^\dagger from lowering operators. The contractions become $U \propto a \cdot b^\dagger \equiv c^\dagger \cdot b^\dagger$ and $U^\dagger \propto a^\dagger \cdot b \equiv c \cdot b$. The contractions of flavor indices can be thought of as gauging a $U(M)$ symmetry. If we also include the left Lie algebra action of $U(N)$ and the action on the right, we get that the degrees of freedom on a link are charged under a $U(N)_L \times U(M) \times U(N)_R$ symmetry. In this way the c^\dagger operators are in the $(N, \bar{M}, 1)$ representation and the b^\dagger are in the $(1, M, \bar{N})$ representation. The composite $c^\dagger \cdot b^\dagger$ transforms in the $(N, 1, \bar{N})$ representation, exactly as the variable U does. The advantage is that in this setup the standard vacuum of the b, c fermions is neutral with respect to all the symmetries, and in particular, it is invariant under $U(M)$, so it is a gauge invariant state. We can reach other gauge invariant states by acting on this state with gauge invariant operators under the $U(M)$, namely, the U, U^\dagger matrix elements. Let us call this standard vacuum $|\Omega\rangle$. Notice that $U^\dagger |\Omega\rangle = 0$, so U, U^\dagger act very asymmetrically on the reference state $|\Omega\rangle$. The complete set of states is built by acting with many U operators. Notice that the U operators commute with each other, so they act as if they are commuting bosonic generators.

The Hilbert space obtained this way can be decomposed into representations of $U(N) \times U(N)$. A state which is algebraically like $U^n |\Omega\rangle$ will have n upper indices with respect to $U(N)_R$ and n lower indices with respect to the left $U(N)_L$. Because of the bosonic statistics, permutations of upper indices can be undone by a change in the order of the product, so long as the permutation is turned over to the lower indices. Projecting into different representations is done by these permutations, and it corresponds to a Young diagram representation with n boxes. The diagram for the lower indices is the same, but since the indices are lowered, we get the conjugate representation. In the intermediate flavor index, the fermionic statistics requires transposing the Young diagram. This argument appeared in [15] (see also [16] and references therein). The Hilbert space is therefore decomposed into the sum of tensor products or representations of $U(N)$ and their conjugates, where each representation is classified by a Young diagram.

$$Hilb \sim \bigoplus_Y (\bar{R}_Y \otimes R_Y) \sim \bigoplus_Y Hilb(Y) \quad (12)$$

and Y is a Young diagram (tableau). For example,

$$Y(5, 3, 2) = \begin{array}{|c|c|c|c|c|} \hline \square & \square & \square & \square & \square \\ \hline \square & \square & \square & & \\ \hline \square & \square & & & \\ \hline \end{array}$$

Here in the Hilbert space, each summand is represented by one copy of the Young diagram for the upper indices let's say, with the understanding that the conjugate representation is giving the representation of the other $U(N)$ in the lower index structure.

Our goal is to show that when $M \rightarrow \infty$ we should recover the Hilbert space of the original U variables that would enter in the Kogut-Susskind formulation.

In that formulation, the entries of the matrices U , as operators, are scalar functions of the group elements. These also commute with each other and their polynomials generate the space of L^2 functions on the group manifold $U(N)$. The Hilbert space $L^2(G)$ itself is given by the following definition. We need wave functions from the group manifold to the complex numbers

$$\psi : G \rightarrow \mathbb{C} \tag{13}$$

and the norm is given by

$$\langle \psi | \psi \rangle = \int \psi^*(g) \psi(g) dg \tag{14}$$

where dg is the Haar measure on the group manifold (this is the unique group invariant measure on G). The trivial function $\psi(g) = 1$ is group invariant. All other wave functions can be obtained from this one by polynomials in the U, U^{-1} matrix component functions and then taking the L^2 completion.

So we need to show that when we take $M \rightarrow \infty$ in the quantum link formulation, we can recover this Hilbert space, $L^2(U(N))$. The constant function 1 on the group plays the role of the vacuum $|0\rangle$ in $L^2(U(N))$. The excited states are described by harmonic functions on $U(N)$. On $L^2(U(N))$, both U and U^\dagger act non-trivially on the vacuum, whose actions are different than the actions we have on the fermion reference vacuum state $|\Omega\rangle$. For any Lie group G , we can now appeal to the Peter-Weil theorem. This theorem states that when we decompose $L^2(G)$ into representations of the left and right symmetries of group multiplication, and we get that $G_L \times G_R$ is decomposed into a direct sum of products of representations

$$L^2(G) = \bigoplus_R \bar{R} \otimes R. \tag{15}$$

Let us look at how one of these pairs of Tableaux, denoting a single representation, can be represented graphically. For example, in $U(5)$, we can take

The second tableaux with the filled boxes is the one of anti-boxes. It is turned by 180 degrees and put at the bottom of the diagram. The total vertical size is N (in this case 5). The constraint is such that the two tableaux do not overlap horizontally.

$$|0\rangle \equiv \begin{array}{|c|c|c|c|} \hline & & & \\ \hline & & & \\ \hline & & & \\ \hline & & & \\ \hline \end{array} \quad (17)$$
[illegible]

Notice also that the representations of $SU(N)$ that appear on both the $L^2(G)$ and the fermion representation have the same dimension. To get the $U(1)$ charge correctly for $L^2(U(N))$ in the fermion formulation, what we have done in practice is that we shifted the $U(1)$ charge so that the new vacuum has trivial charge. Happily, we see that we can match the representations of $U(N)$ with a few boxes. These are the representations with small Casimir. The constraint on M tells us that the maximum width of the fermion Tableaux is M , so that to recover the Hilbert space of $L^2(U(N))$ we need to take $M \rightarrow \infty$ and shift the charge enough so that the room on the left to remove boxes is as large as needed. The most symmetric way to do this is to choose $K = M/2$.

This shows that at least relative to the new ground state, we recover the representation of the Hilbert space we want, namely $L^2(U(N))$ with a cutoff that depends on M . The gauge invariance relative to the flavor $U(M)$ shows we have no additional states to worry about. Computing matrix elements of U , U^\dagger between states is beyond the scope of the present work and will be taken in more detail in a future publication.

3 Target $U(1)$ Quantum Rotor

In order to test the fidelity of our $U(1)$ qubit representations, we compare to the full $U(1)$ quantum rotor,

$$H = \frac{g^2}{2} E^2 + \frac{1}{g^2} (2 - U - U^\dagger) \quad (19)$$

with symplectic algebra

$$[E, U] = U, \quad [E, U^\dagger] = -U^\dagger, \quad [U, U^\dagger] = 0 \quad (20)$$

This can be truncated by a cutoff in either the flux basis ($|\ell\rangle$ or the field basis $|\theta\rangle$). We will subsequently show that the multi-flavor D-theory construction can be reformulated to exactly reproduce the flux cutoff L of this rotor with $M = 2L$ flavors and therefore converge exactly to the full rotor in the $M \rightarrow \infty$ limit.

It is convenient to rescale the Hamiltonian by $1/g^2 = \sqrt{h/2}$ so that

$$H = -\frac{1}{2} \partial_\theta^2 + \frac{h}{2} (2 - 2 \cos \theta) \quad (21)$$

The flux representation is of course just the Fourier transforms, $\langle \ell | \theta \rangle = \exp(i\ell\theta)$, with the delta function normalized states $U|\theta\rangle = \exp(i\theta)|\theta\rangle$, or in the flux basis, $E|\ell\rangle = \ell|\ell\rangle$. Explicitly writing the matrix representation of the Hamiltonian in this basis,

$$\langle \ell' | H | \ell \rangle = \frac{\ell^2}{2} \delta_{\ell', \ell} + \frac{h}{2} (2\delta_{\ell', \ell} - \delta_{\ell'+1, \ell} - \delta_{\ell'-1, \ell}) \quad (22)$$

with $\ell = 0, \pm 1, \pm 2, \dots$. This leads to a natural approximation for the infinite dimensional Hilbert space by restricting the flux to $\ell \in [-L, L]$ ⁴. It is the pathway that the D-theory pursues. To illustrate, let us write down the matrices of the operators for the $L = 2$ state case:

$$\hat{U} \rightarrow U_L = \begin{bmatrix} 0 & 1 & 0 & 0 & 0 \\ 0 & 0 & 1 & 0 & 0 \\ 0 & 0 & 0 & 1 & 0 \\ 0 & 0 & 0 & 0 & 1 \\ 0 & 0 & 0 & 0 & 0 \end{bmatrix}, \quad \hat{E} \rightarrow E_2 = \begin{bmatrix} -2 & 0 & 0 & 0 & 0 \\ 0 & -1 & 0 & 0 & 0 \\ 0 & 0 & 0 & 0 & 0 \\ 0 & 0 & 0 & 1 & 0 \\ 0 & 0 & 0 & 0 & 2 \end{bmatrix} \quad (23)$$

The field truncation is more subtle. One can of course discretize the field to the Z_N clock model with $\theta = 2\pi(0, 1, \dots, N-1)/N$ and choose again to restrict flux $\ell \in [-L, L]$ with a cyclic generator E for the Z_N subgroup. Illustrating the $N = 5$ state truncation, the operators are

$$U \rightarrow U_{Z_N} = \begin{bmatrix} 0 & 1 & 0 & 0 & 0 \\ 0 & 0 & 1 & 0 & 0 \\ 0 & 0 & 0 & 1 & 0 \\ 0 & 0 & 0 & 0 & 1 \\ 1 & 0 & 0 & 0 & 0 \end{bmatrix}, \quad \hat{E} \rightarrow E_2 = \begin{bmatrix} -2 & 0 & 0 & 0 & 0 \\ 0 & -1 & 0 & 0 & 0 \\ 0 & 0 & 0 & 0 & 0 \\ 0 & 0 & 0 & 1 & 0 \\ 0 & 0 & 0 & 0 & 2 \end{bmatrix} \quad (24)$$

Note that the electric fields are identical but the fields are different. The D-theory approach preserves the symplectic algebra $[E, U] = U$ and $[E, U^\dagger] = -U^\dagger$ but breaks the unitarity $U^\dagger U = 1$, whereas the clock model does the opposite, preserving $U^\dagger U = 1$ but not the commutator algebra. Preserving both leads to an infinite-dimensional Hilbert space, which is exactly what we need to avoid⁵.

⁴The Casimir of the charge state is ℓ^2 , so this is also a cutoff on the maximum value of the Casimir.

⁵As a side note, the clock model is the quantization one gets by using a two-torus cylinder geometry, rather than the sphere. The algebra is then very similar to that of a fuzzy torus, but with this choice of E there is a discontinuity of the classical variable at the gluing of the upper and lower part of the cylinder that avoids a doubling of low energy degrees of freedom.

In the flux truncation (i.e. D-theory), the fields obey,

$$[UU^\dagger]_{\ell',\ell} = \delta_{\ell',\ell} - \delta_{\ell',-L}\delta_{\ell,-L} \quad , \quad [U^\dagger U]_{\ell',\ell} = \delta_{\ell,\ell'} - \delta_{\ell',L}\delta_{\ell,L} \quad (25)$$

with the non-zero commutator

$$[U, U^\dagger]_{\ell',\ell} = \delta_{\ell',L}\delta_{\ell,L} - \delta_{\ell',-L}\delta_{\ell,-L} \quad (26)$$

Notice that these are concentrated on the largest ℓ exclusively, so they can be considered as only living in the UV (high energy regime) of the model, keeping the infrared physics roughly the same.

In Sec. 5, we compare the low spectrum as a function of h in the strong coupling limit $h = 0$ and the weak coupling limit $h = \infty$. We show that the low spectra is of course exact at $h = 0$ and is remarkably accurate for a large range of values of $h = 1/g^4$ even for a $L = 2$ or $L = 4$ flux cutoff. This appears to be remarkable or even paradoxical since for the flux truncation, the field variables obey the nilpotency $U^{2L+1} = 0$ and therefore have exactly degenerate zero eigenvalues. This would seem to be a poor stating point in comparison with the eigenvalues of the clock model $e^{2\pi\ell/(2L+1)}$. The point is that U, U^\dagger are not observables in the flux truncation: they are not Hermitian and they are also not normal matrices. In that sense, their eigenvalues are not the results of quantum measurements in the Hilbert space. The situation is better for the combinations such as $U + U^\dagger$ which do correspond to Hermitian operators as illustrated in Fig. 1. On the left (Fig. 1), we observe a nearly harmonic oscillator low spectra (orange) for the D-theory even for $L = 3$. In the clock model, U, U^\dagger are normal, so both their real and imaginary parts are Hermitian matrices that commute and can be diagonalized simultaneously. Hence, their eigenvalues can be measured simultaneously and we can use that double measurement to determine the phases $e^{2\pi k/(2L+1)}$. On the right (Fig. 1) this is used to show a remarkable match for D-theory for all angles even at a small cutoff $L = 8$.

Note also that the field truncation with only discrete symmetry surviving has no natural generalization to non-Abelian groups; there is no infinite sequence of finite discrete subgroups that uniformly populate their manifolds. For example for $SU(2)$, the largest such finite group that is uniform on $SU(2)$ is the 120-element icosahedral group, and it is known that it fails to be in the universality class of the two-color gauge theory [18].

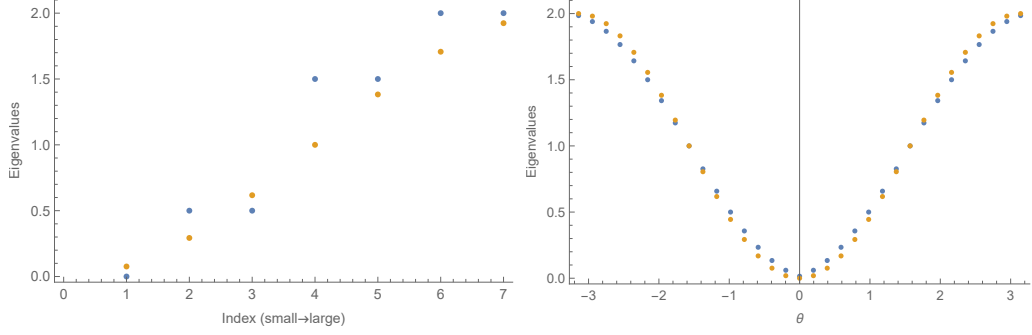


Figure 1: On the left for $L = 3$, the 7 eigenvalues for the clock model (blue) potential $V(\theta) = 1 - \cos(\theta)$ are compared to the eigenvalues of the D-theory (orange) potential $\hat{V} = 1 - (\hat{U} + \hat{U}^\dagger)/2$. On right, the clock model (blue) eigenvalues $V(\pi m/L)$ are mapped to $\theta \in [-\pi, \pi]$ compared with the D-theory spectra (orange) for $L = 8$ duplicated by reflection: $\theta \rightarrow -\theta$.

4 Complexity of qubit Realizations

We now turn to our multi-flavor framework with D-theory rotor Hamiltonian Eq. (19) with \hat{U} and \hat{U}^\dagger given by a direct sum over the M flavors:

$$\hat{U}_{sum}^\dagger = \sum_{m=1}^M a_m^\dagger b^m, \quad \hat{U}_{sum} = \sum_{m=1}^M b_m^\dagger a^m \quad (27)$$

acting on $2M$ fermionic fock space with the field of dimension 4^M . We note that the fermionic operators imply that the nilpotency $\hat{U}^{M+1} = 0$ which coincides with the flux truncation with $M = 2L$. However, we will see that it does not represent the same matrices for this truncation. The M -flavor fermionic Quantum Link form starts in a 4^M dimensional Hilbert space (each fermion has a two-dimensional Hilbert space), but if we impose the half-filling condition for each flavor due to the fermion number conservation as

$$a^{\dagger m} a_m + b_m^\dagger b^m = 1 \text{ (No sum)} \quad (28)$$

we are now in Hilbert space of dimension 2^M allowing us to represent the operators as M hard boson (or sigma matrix) qubits. The point to be made is that in the sums Eq. (27), only terms that preserve each of all of these individual fermion number combinations of $a + b$ appear, so they can be diagonalized ahead of computations.

These actually generate a subgroup of the original $U(M)$ flavor symmetries which are flavor diagonal (that is, this is a set of $U(1)^M$ generators that has been fixed).

In this subspace, for each flavor, we have the isometric mapping

$$\{a^\dagger b, b^\dagger a, a^\dagger a - b^\dagger b\} \rightarrow \{\sigma^+, \sigma^-, \sigma^z\} \quad (29)$$

and there are no fermion statistics in the σ on the right. We have in this way eliminated the need to do any Jordan-Wigner transformations to convert fermions into qubits.

In this form, the full representation of $SU(2)$ available by these M flavors is $\bigotimes_{m=1}^M \mathbf{2}$. This representation is reducible, and its irreducible decomposition contains the irreducible $\mathbf{M} + \mathbf{1}$ representation which we need to match the flux truncation Hamiltonian in Eq. (23). For example, for the $M = 4$ case, the decomposition of the full $\bigotimes_{m=1}^4 \mathbf{2}$ representation contains the irreducible $\mathbf{5}$ representation as

$$\bigotimes_{m=1}^4 \mathbf{2} = \mathbf{1} \oplus \mathbf{1} \oplus \mathbf{3} \oplus \mathbf{3} \oplus \mathbf{3} \oplus \mathbf{5} \quad (30)$$

$$\square \otimes \square \otimes \square \otimes \square = \begin{array}{|c|c|} \hline \square & \square \\ \hline \square & \square \\ \hline \end{array} \oplus \begin{array}{|c|c|} \hline \square & \square \\ \hline \square & \square \\ \hline \end{array} \oplus \begin{array}{|c|c|c|} \hline \square & \square & \square \\ \hline \square & \square & \square \\ \hline \end{array} \oplus \begin{array}{|c|c|c|} \hline \square & \square & \square \\ \hline \square & \square & \square \\ \hline \end{array} \oplus \begin{array}{|c|c|c|c|} \hline \square & \square & \square & \square \\ \hline \square & \square & \square & \square \\ \hline \end{array}$$

Figure 2: The Young tableau representation of the $SU(2)$ irreducible decomposition Eq. (30) (bottom row). Each box corresponds to an index of the tensor representation of the wavefunction. Especially, two boxes aligned in a column correspond to the indices of the Levi-Civita tensor ϵ^{ij} , and hence they have no degree of freedom. We can embed the $U(1)$ Hamiltonian (Eq. (19)) with the flux cutoff of $L = 2$ (i.e. the five-dimensional representation of $U(1)$) into the symmetric representation $\mathbf{5}$ of $SU(2)$, which is represented as the last term of the right hand side (the four boxes aligned in a single row).

The simplifications where we start with $2M$ fermion qubits and end up with only M qubits encodes an $M + 1$ dimensional Hilbert space inside a 2^M dimensional Hilbert space. We have cut the number of qubits by half with the half-filling condition. Still, the dimension of the Hilbert space where our physics is encoded grows exponentially with the number of states. We will name this property an *exponential format*.

The Hilbert space on which the $\mathbf{M} + \mathbf{1}$ representation acts is spanned by the states that are totally symmetric on the flavor symmetry, i.e. the states

$$|m\rangle = \sum_{\{\pi(M,m)\}} \binom{M}{m}^{-1} |1\rangle_{\pi(1)} |1\rangle_{\pi(2)} \cdots |1\rangle_{\pi(m)} |0\rangle_{\pi(m+1)} \cdots |0\rangle_{\pi(M)} \quad (31)$$

for $m = 0, \dots, M$, where $\{\pi(M, m)\}$ is the set of all possible partitions of M integers to a group of m and the other of $M - m$ ⁶. In this sense, if we gauge the permutation symmetry of the qubits, we get the unique representation of dimension $2L + 1$. This can be justified by the gauging of the $U(M)$ flavor symmetry of the original D-theory formulation. The combinations in Eq. (29) are invariant only under a $U(1)^M$ subgroup of $U(M)$ rather than the full $U(M)$. The individual σ_z are linear combinations of the Cartan generators. The commutant of $U(1)^M$ inside $U(M)$ also includes the permutations of the $U(1)$, which should also be gauged. This justifies this prescription for keeping only the symmetric states.

The ingredients for the construction of the qubit Hamiltonian are the Cartan-Weyl basis operators $\hat{L}_+ = \hat{L}_x + i\hat{L}_y$, $\hat{L}_- = \hat{L}_x - i\hat{L}_y$, and \hat{L}_z in the $\mathbf{M} + \mathbf{1}$ irreducible representation of $SU(2)$, i.e. the spin- $M/2$ operators. This truncation of the $U(1)$ fields with the spin- $M/2$ operators is investigated by Zhang et al. [12] to study the effect of this spin truncation to the BKT phase transition of the $O(2)$ model. We can express these Cartan-Weyl basis operators in the full $\bigotimes_{m=1}^M \mathbf{2}$ representation, i.e. in the M -qubit representation as

$$\hat{U}_{\text{sum}}^\dagger \rightarrow \hat{L}_+ = \frac{1}{\sqrt{(M/2)(M/2 + 1)}} \sum_{m=1}^M \sigma_m^+, \quad (32)$$

$$\hat{U}_{\text{sum}} \rightarrow \hat{L}_- = \frac{1}{\sqrt{(M/2)(M/2 + 1)}} \sum_{m=1}^M \sigma_m^-, \quad (33)$$

$$\hat{E}_{\text{sum}} \rightarrow L_z = \frac{1}{2} \sum_{m=1}^M \sigma_m^z \quad (34)$$

The normalization factors of \hat{L}_\pm are given so that their actions on the $|0\rangle$ state match with those of the original U operators, and hence the low spectra of the qubit

⁶In the usual spin notation, we have that $m = j_z + j$, where j is the spin of the representation and j_z is the z eigenvalue of angular momentum.

Hamiltonian replicate those of the continuum Hamiltonian in the small h region. The action of the \hat{L}_+ and \hat{L}_- operators are to raise and lower the state, respectively, as

$$\hat{L}_+ |m\rangle = \frac{\sqrt{(m+1)(M-m)}}{\sqrt{(M/2)(M/2+1)}} |m+1\rangle, \quad \hat{L}_- |m\rangle = \frac{\sqrt{m(M-m+1)}}{\sqrt{(M/2)(M/2+1)}} |m-1\rangle \quad (35)$$

and the \hat{L}_z operator is the shifted number operator $\hat{L}_z |m\rangle = (m - M/2) |m\rangle$. Since the commutation relations of \hat{L}_+ and \hat{L}_- with \hat{L}_z are

$$[\hat{L}_z, \hat{L}_+] = \hat{L}_+, \quad [\hat{L}_z, \hat{L}_-] = -\hat{L}_- \quad (36)$$

which match with Eq. (20), whereas the commutator of \hat{L}_+ and \hat{L}_- is \hat{L}_z which violates the last relation of Eq. (20). If we consider the mapping $E \rightarrow \hat{L}_z$, $U \rightarrow \hat{L}_+$, and $U^\dagger \rightarrow \hat{L}_-$, the Hamiltonian

$$\hat{H}_{\text{qubit}} = \frac{g^2}{2} \hat{L}_z^2 - \frac{1}{2g^2} (\hat{L}_+ + \hat{L}_-) \quad (37)$$

has the same symmetry as the continuum Hamiltonian Eq. (19) does (more precisely, the different pieces in the Hamiltonian have the same algebra).

4.1 Phase space considerations.

One can try to understand this a little bit better from the point of view of Hamiltonian classical mechanics on the phase space of the cylinder and the sphere. The reason to do so is to understand better the relation between both dynamical systems.

Basically, after turning to the problem of writing in terms of qubits and focusing on the correct gauge invariant states, the original problem is reduced to the study of a single copy of the $SU(2)$ Lie algebra hiding in the big Hilbert space. It is the physics of this sub-Hilbert space that we want to analyze by classical methods to get an intuition.

On the cylinder (the tangent bundle on the circle), we have variables α (the periodic variable) and p_α , with the Poisson bracket $\{\alpha, p_\alpha\} = 1$. The cylinder Hamiltonian is

$$H = \frac{1}{2} p_\alpha^2 - h \cos(\alpha) \quad (38)$$

By contrast, on the sphere we have a pair of spherical coordinates $\tilde{\theta}$, $\tilde{\phi}$, with $\tilde{\phi}$ periodic and with the Poisson bracket $\{\tilde{\phi}, \tilde{\theta}\} = A/(\sin(\tilde{\theta}))$ (this is the inverse of the volume form in spherical coordinates, up to a rescaling factor, which we have called A). The conjugate variable to $\tilde{\phi}$ is actually $p_{\tilde{\phi}} = \cos(\tilde{\theta})/A$ rather than $\tilde{\theta}$. In the rectangular coordinates, this is the z coordinate, and that is identified with L_z after rescaling. On the other hand, $L^+ \propto \sin(\tilde{\theta}) \exp(i\tilde{\phi})$, which is identified with $\sqrt{1 - z^2} \exp(i\phi) \sim \sqrt{1 - L_z^2/L^2} \exp(i\tilde{\phi})$. That is, the Hamiltonian will look as follows when we take the classical identification $\alpha \equiv \tilde{\phi}$, which results from taking the classical periodicity of the variables into account. If we include the constraint $L_x^2 + L_y^2 = L^2 - L_z^2$, where L^2 is a c-number, we find that the Hamiltonian actually takes the form

$$H = \frac{1}{2}p_\alpha^2 - h\sqrt{1 - p_\alpha^2/p_{\max}^2} \cos(\alpha) \quad (39)$$

For this to work, we need to have $p_\alpha = L_z$, $p_{\max} = L$ and $A = 1/p_{\max} = 1/L$, so that $p_\alpha = p_{\max} \cos(\theta)$. The normalization of the naive kinetic term has been scaled to match what we need.

We can now expand in powers of $1/p_{\max}$ and we get that

$$H = \frac{1}{2}p_\alpha^2 - h \cos(\alpha) + \frac{h}{2} \frac{p_\alpha^2}{p_{\max}^2} \cos(\alpha) + \dots \quad (40)$$

so when we take $p_{\max} \rightarrow \infty$, we recover the cylinder Hamiltonian. At finite p_{\max} , there are what should be interpreted as higher derivative corrections in the Hamiltonian. These are suppressed by the cutoff p_{\max} . The quantization of this system leads to the quantum Hamiltonian Eq. (37), provided that $1/g^4 \propto h/p_{\max}$. Here, we need to remember that L_+ , L_- , L_z have roughly the same normalization. One can say that the quantity $1/p_{\max}$ is playing the role of \hbar in a quantum expansion. This is also related to the volume of phase space, which is computed to be proportional to $p_{\max} \simeq (2L+1)$ in the Planck units.

In a field theory setup, these higher derivative corrections are expected to be irrelevant perturbations, at least by naive power counting: they affect the UV dynamics, but should flow to the same universality class in the infrared. These scale like the electric field squared, times the magnetic field squared (the naive plaquette). In that vein, the low energy spectrum of Eq. (37) should converge to the low energy spectrum of the Kogut-Susskind Hamiltonian with the normalization of the equation Eq. (21) when we take the cutoff to infinity as well.

One can try to understand a similar idea for more general groups that are not just $U(1)$. As argued earlier, we should study the quantization of the Grassmannian $\mathbb{G}(N, 2N)$, when we are discussing $U(N)$ links which are where the coherent states of [5] take values. One would then try to understand how to take the semiclassical double scaling limit correctly to get a *cylinder over $U(N)$* , namely, the tangent space of $U(N)$ as a phase space, with a Hamiltonian and a parameter playing the role of p_{\max} . This type of analysis is beyond the scope of the present work.

4.2 Exponential Formats

The Hamiltonians Eq. (19) and Eq. (37) are not exactly the same due to the difference between the coefficients of the actions of the raising and lowering operations. In the flux truncation, they are always constant (normalized to 1), and those in $SU(2)$ which are not constant but rather depend on the target state as we saw in Eq. (35). This is also true in the classical limit described by Eq. (40), where there are higher derivative corrections to the Hamiltonian. Also, remember that the Hamiltonian Eq. (37) acts on a Hilbert space of large dimension 2^M , but that only the states in the $\mathbf{M} + 1$ irreducible representation matter and are invariant under all constraints. We dubbed this property as being an exponential format, where the dimension of the Hilbert space grows exponentially in the number of states we need.

We can try to do better at the level of matching the operators in the subspace of interest in the total Hilbert space, by adding corrections to the quantum Hamiltonian that get rid of the differences at finite cutoff. This should be equivalent to adding (or depending on the point of view, subtracting) irrelevant operators to compensate for the differences in the formulation.

To construct the U and U^\dagger with our qubit construction, we may use one of the two ansatze:

$$\hat{U}' = \sum_{k=0}^{M/2-1} a_k \hat{L}_z^k \hat{L}_+ \hat{L}_z^k, \quad \hat{U}'' = \sum_{k=0}^{M/2-1} b_k (\hat{L}_+ \hat{L}_-)^k \hat{L}_+ \quad (41)$$

The first one, for what we call U' can also be thought of as having L_z/L_{\max} corrections to U^+ , as one would expect from the higher derivative expansion Eq. (40). As such, the coefficients should be suppressed by the powers of $1/L_{\max}^{2k}$, up to normal ordering ambiguities.

One can compute the coefficients a_k or b_k so that the action of \hat{U}' or \hat{U}'' is the same as U in Eq. (19). For the first \hat{U}' for example, the action of each $\hat{L}_z^k \hat{L}_+ \hat{L}_z^k$ operator is as

$$\hat{L}_z^k \hat{L}_+ \hat{L}_z^k |m\rangle = ((m - M/2 + 1)(m - M/2))^k \frac{\sqrt{(m+1)(M-m)}}{\sqrt{(M/2)(M/2+1)}} |m+1\rangle \quad (42)$$

Hence, the coefficients a_k can be computed by solving the linear equation

$$\sum_{k=0}^{M/2-1} A_{mk} a_k = 1 \quad (43)$$

where A_{mk} is a $(M/2) \times (M/2)$ -dimensional matrix with elements of $A_{mk} = ((m - M/2 + 1)(m - M/2))^k \sqrt{(m+1)(M-m)} / \sqrt{(M/2)(M/2+1)}$ where the indices m and k run from 0 to $M/2 - 1$.

For the other case of \hat{U}'' , we need to solve the linear equation $\sum_{k=0}^{M/2-1} B_{mk} b_k = 1$ where $B_{mk} = ((m+1)(M-m))^{k+1/2} / \sqrt{(M/2)(M/2+1)}$. Once we choose a_k and b_k appropriately, the operators \hat{U}' and \hat{U}'' can be identical in the space spanned by the states Eq. (31), even though they are not in the full M -qubit space.

Since the values of A_{mk} and B_{mk} grow exponentially with k , the values of a_k and b_k are expected to decay exponentially for higher k terms. Actually, [12] numerically shows that a_k decays exponentially with k . For small cutoff $L = 1, 2, 3$, the \hat{U}' operator can be constructed as

$$\begin{aligned} \hat{U}'_{L=1} &= \hat{L}_+ \\ \hat{U}'_{L=2} &= \hat{L}_+ + \left(-\frac{1}{2} + \frac{\sqrt{6}}{4} \right) \hat{L}_z \hat{L}_+ \hat{L}_z \\ \hat{U}'_{L=3} &= \hat{L}_+ + \left(-\frac{2}{3} - \frac{\sqrt{2}}{12} + \frac{3\sqrt{30}}{20} \right) \hat{L}_z \hat{L}_+ \hat{L}_z + \left(\frac{1}{12} + \frac{\sqrt{2}}{24} - \frac{\sqrt{30}}{40} \right) \hat{L}_z^2 \hat{L}_+ \hat{L}_z^2 \end{aligned} \quad (44)$$

and the \hat{U}'' operator can be constructed as

$$\begin{aligned}
\hat{U}_{L=1}'' &= \hat{L}_+ \\
\hat{U}_{L=2}'' &= \left(3\sqrt{\frac{3}{2}} - 2\right) \hat{L}_+ + \left(\frac{1}{2} - \frac{\sqrt{6}}{4}\right) \hat{L}_+ \hat{L}_- \hat{L}_+ \\
\hat{U}_{L=3}'' &= \left(5 - 9\sqrt{\frac{6}{5}} + 5\sqrt{2}\right) \hat{L}_+ + \left(-\frac{3}{4} - \frac{11\sqrt{2}}{12} + \frac{9\sqrt{30}}{20}\right) \hat{L}_+ \hat{L}_- \hat{L}_+ \\
&\quad + \left(\frac{1}{12} + \frac{\sqrt{2}}{24} - \frac{\sqrt{30}}{40}\right) (\hat{L}_+ \hat{L}_-)^2 \hat{L}_+
\end{aligned} \tag{45}$$

For the expressions of U' , notice that numerically we have that $-1/2 + \sqrt{6}/4 \sim 0.11$, and $-2/3 - \sqrt{2}/12 + 3\sqrt{30}/20 \sim 0.049 \sim (2/3)^2 * (0.11)$ is roughly the suppression one would expect in terms of $1/p_{\max}^2$ counting.

The point is that if our goal is to produce the flux truncated Kogut-Susskind Hamiltonian on the nose, it can be done. Ideally, one would actually use L^+, L^- instead and try to argue that one is in the same universality class. The main reason is that the Hamiltonian Eq. (37) is made of sums of products of only two sigma matrices. These can be readily implemented as 2 qubit gates, perhaps with some swaps of qubits. Therefore, it provides a more efficient implementation on a NISQ device, where reducing the number of total gate operations per qubit is essential to get to a result that one can trust, before one loses coherence on the device.

4.3 Linear Formats and Sparsity

The formulation we have used to construct the qubit Hamiltonian with links in Eqs. (45) and (46) requires at least $M = 2L$ qubits, discarding all other representations in the irreducible decomposition of $\bigotimes_{\alpha=1}^M \mathbf{2}$ than the $\mathbf{M} + \mathbf{1}$ representation. For large L , the Hilbert space grows exponentially in L losing completely the *quantum advantage*. We now introduce another qubit representation with which one can store information with only a logarithmic number of qubits, using M qubits to represent the $M + 1$ -dimensional Hilbert space.

One needs only $N_{\min} = \lceil \log_2(M+1) \rceil$ qubits by keeping the other representations by mapping the $|0\rangle, |1\rangle, \dots, |M\rangle$ states to the computational basis states as

$$|m\rangle \rightarrow |b_{N_{\min}}\rangle \otimes |b_{N_{\min}-1}\rangle \otimes \dots \otimes |b_1\rangle \otimes |b_0\rangle \quad (46)$$

where $b_{N_{\min}}b_{N_{\min}-1}b_1b_0$ is the binary representation of m . In this encoding, the dimension of the Hilbert space in which we embed our problem grows linearly with the dimension of Hilbert space we want to encode. We would call this a linear format. Notice that this setup starts with the truncation and tries to fit it into a Hilbert space in an arithmetic way without starting with the symmetry algebra first. It is more economical in terms of qubits, but the generalization to non-Abelian fields for even a polynomial format is not straight forward, and even if possible presents a challenging research project in qubit algebra [19].

We begin by introducing a M -bit quantum adder [20]:

$$A = \sigma_0^+ + \sigma_1^+ \sigma_0^- + \sigma_2^+ \sigma_1^- \sigma_0^- + \dots + \sigma_{N_{\min}-1}^+ \sigma_{N_{\min}-1}^- \dots \sigma_1^- \sigma_0^- \quad (47)$$

which maps the computational basis states as $|m\rangle \rightarrow |m+1, N_{\min}\rangle \bmod 2^M$. Then, the adder can be modified to represent the raising operator \hat{U}_{\min} replacing the mod by annihilation for the highest state as $\hat{U}_{\min}|M\rangle = 0$. To do this in general, we multiply the projector P from right to A , where P is defined to act as the identity for the $|0\rangle, \dots, |M-1\rangle$ states and vanish at least the state $|M\rangle$ and possibly also the higher states. For $M = 2(L = 1)$, for example, using the 3-dimensional subspace of the 2-qubit space with a mapping given as

$$|0\rangle \mapsto |00\rangle, |1\rangle \mapsto |01\rangle, |2\rangle \mapsto |10\rangle \quad (48)$$

The \hat{U}_{\min} , \hat{U}_{\min}^\dagger , and the corresponding \hat{E}_{\min} operator are expressed as

$$\hat{U}_{\min} = AP = \frac{1}{2}\sigma_0^+ + \sigma_1^+ \sigma_0^- + \frac{1}{2}\sigma_1^3 \sigma_0^+ \quad (49)$$

$$\hat{U}_{\min}^\dagger = P^\dagger A^\dagger = \frac{1}{2}\sigma_0^- + \sigma_1^- \sigma_0^+ + \frac{1}{2}\sigma_1^3 \sigma_0^- \quad (50)$$

$$\hat{E}_{\min} = -\frac{1}{2}\sigma_1^3 - \frac{1}{2}\sigma_1^3 \sigma_0^3 \quad (51)$$

given that one of the possible choices of the projector P is

$$P = I - (I - \sigma_1^3)(I - \sigma_0^3)/4 \quad (52)$$

For another example of $M = 4(L = 2)$, using the 5-dimensional subspace of the 3-qubit space with a mapping given as

$$|0\rangle \mapsto |000\rangle, |1\rangle \mapsto |001\rangle, |2\rangle \mapsto |010\rangle, |3\rangle \mapsto |011\rangle, |4\rangle \mapsto |100\rangle \quad (53)$$

the \hat{U}_{\min} , \hat{U}_{\min}^\dagger , and the corresponding \hat{E}_{\min} operator are expressed as

$$\hat{U}_{\min} = AP = \frac{1}{2}\sigma_0^+ + \frac{1}{2}\sigma_1^+\sigma_0^- + \frac{1}{2}\sigma_2^3\sigma_0^+ + \frac{1}{2}\sigma_2^3\sigma_1^+\sigma_0^- + \sigma_2^+\sigma_1^-\sigma_0^- \quad (54)$$

$$\hat{U}_{\min}^\dagger = P^\dagger A^\dagger = \frac{1}{2}\sigma_0^- + \frac{1}{2}\sigma_1^-\sigma_0^+ + \frac{1}{2}\sigma_2^3\sigma_0^- + \frac{1}{2}\sigma_2^3\sigma_1^-\sigma_0^+ + \sigma_2^-\sigma_1^+\sigma_0^+ \quad (55)$$

$$\hat{E}_{\min} = -\frac{1}{4}\sigma_1^3 + \frac{1}{4}\sigma_1^3\sigma_0^3 - \frac{1}{2}\sigma_2^3 - \frac{1}{2}\sigma_2^3\sigma_0^3 - \frac{3}{4}\sigma_2^3\sigma_1^3 - \frac{1}{4}\sigma_2^3\sigma_1^3\sigma_0^3 \quad (56)$$

given that one of the possible choices of P is

$$P = (I - \sigma_2^3)/2 \quad (57)$$

These operators also satisfy the first two commutation relations of Eq. (20), so the Hamiltonian constructed from these operators

$$\hat{H}_{\min} = \frac{g^2}{2}\hat{E}_{\min}^2 - \frac{1}{2g^2}(\hat{U}_{\min} + \hat{U}_{\min}^\dagger) \quad (58)$$

preserves the original $U(1)$ symmetry. Drawing on the extensive literature on efficient and robust quantum arithmetic [19] should help in designing optimal circuits for this linear formation.

5 Spectral Matching of D-theory Truncation

In this section, we discuss and numerically compare the low spectra of the 0 + 1-D quantum rotor Hamiltonian with the $U(1)$ symmetry defined in Eq. (19) with those with a small flux cutoff L , a discretization of the group manifold of $U(1)$ to Z_N (clock model), and the spin operators L_\pm as \hat{U} operators (quantum link model) as functions of h .

First, we compare the spectra with the very small cutoff of $L = 2$, $N = 5$, $M = 4$ (i.e. with the five-dimensional Hilbert space) and those with a slightly larger cutoff

of $L = 4$, $N = 9$, $M = 8$ (i.e. with the nine-dimensional Hilbert space) (Fig. 3) with the exact spectra. We define a new coefficient τ parameterizing the coupling h as $h = \tau/(1 - \tau)$ allowing us to plot the whole $h \in [0, \infty)$ with the finite $\tau \in [0, 1)$, besides rescaling the Hamiltonian by $\times(1 - \tau)$. From the figures, for all of the truncation approaches, we can see that for the weak coupling h , we do not need a large cutoff L to reach the precise solution, whereas we do for the strong coupling, and the lower eigenenergies converge faster than the higher energies. Let us also note that the spectrum of the clock model deviates from the exact spectrum with smaller h than that with the flux cutoff does.

This quantum rotor has an interesting feature. By expanding the $\cos \theta$ term by θ , we can decompose the Hamiltonian into the quantum harmonic oscillator (QHO) part $H_0 = p^2/2 + h\theta^2/2$ with the momentum $p = -i\partial_\theta$ and the perturbation term $H_1 = h(-\theta^4/4! + \theta^6/6! - \theta^8/8! + \dots)$ which is the higher-order terms of the cosine. In the large h region, the low spectra tend to condensate around $\theta = 0$, which makes the perturbation H_1 and the periodic boundary conditions of θ trivial, so they should illustrate the even-spaced spectra as well as the well-known QHO spectra with $E_n = \sqrt{h}(n + 1/2)$ for $n = 0, 1, 2, \dots$. To see the two truncations can reproduce this QHO-like behavior with large h , we compare the spectra of the Hamiltonians with the truncations with the spectra of the QHO (Fig. 4). These QHO solutions correspond to the topologically trivial trajectories with zero winding (i.e. the topological charge $q = \int_{-\infty}^{\infty} dt (d\phi/dt) = 0$) along the time evolution, whereas the topologically non-trivial ($q \neq 0$) trajectories start to be non-negligible in the small h region once we take the path integral for quantization [21]. Since we need to simulate the behavior with large h , we use larger truncations of $L = 10$, $N = 21$, and $M = 20$. As seen in the figure, the flux truncated Hamiltonian and the clock model well reproduce the QHO spectra in the large h regions until they start to gain the non-negligible errors due to the truncations. However, the spectra computed with the spin truncation are completely off from the QHO spectra, which can be expected given that the dominating potential term $2 - \hat{U} - \hat{U}^\dagger = 2 - \hat{L}_x$ in the large h region has the even spaced eigenvalues of $2 - 2m/\sqrt{(M/2)(M/2 + 1)}$ with $m = -M/2, -M/2 + 1, \dots, M/2 - 1, M/2$ which grow linearly with h . This indicates we need the corrections as we proposed in Sec. 4.2 for h very large. At intermediate h , we cannot neglect the term with L_z^2 and the agreement should be better.

To evaluate the performance of the flux truncation, we can also look at the breaking

of the commutator in the eigenbasis for the low spectrum

$$\langle E_j | [U, U^\dagger] | E_k \rangle \quad (59)$$

which is, without the truncation or with the clock model discretization, exactly zero. For j and k with the same parity, the matrix elements are all zero. The non-zero elements (i.e. j and k with the different parities) for small j and k of this matrix as functions of h with a small cutoff ($L = 2$ and $L = 4$) are as Fig. 5, demonstrating that the effects of the breaking of the commutator on the low energy states are small for smaller j and k , for smaller coupling h , and larger cutoff L . This behavior of the breaking of the zero commutator validates that the flux-truncated Hamiltonian describes the effective theory of the exact $U(1)$ quantum rotor in the small h region.

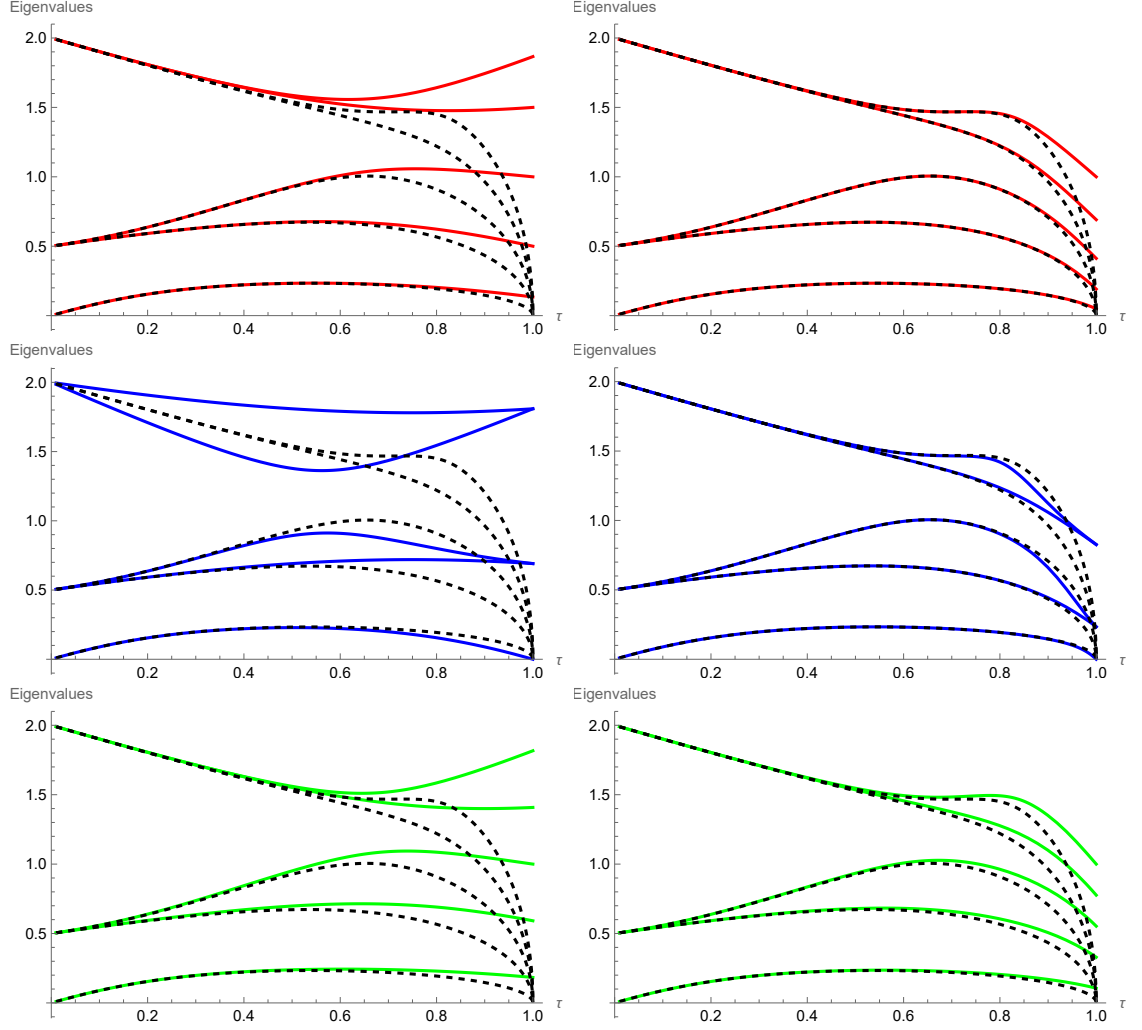


Figure 3: The comparisons of the lowest five eigenvalues as the functions of τ (defined so that $h = \tau/(1-\tau)$) for the quantum rotor Hamiltonian computed with a small flux cutoff (red curves, top left for $L = 2$ and top right for $L = 4$), those computed with the discrete Z_N group or a clock model (blue curves, middle left for $N = 5$ and middle right for $N = 9$), those computed with the spin operators \hat{L}_\pm as the \hat{U} operators (green curves, bottom left for $M = 2L = 4$ and bottom right for $M = 2L = 8$), and those of the exact Hamiltonian (black dotted curves).

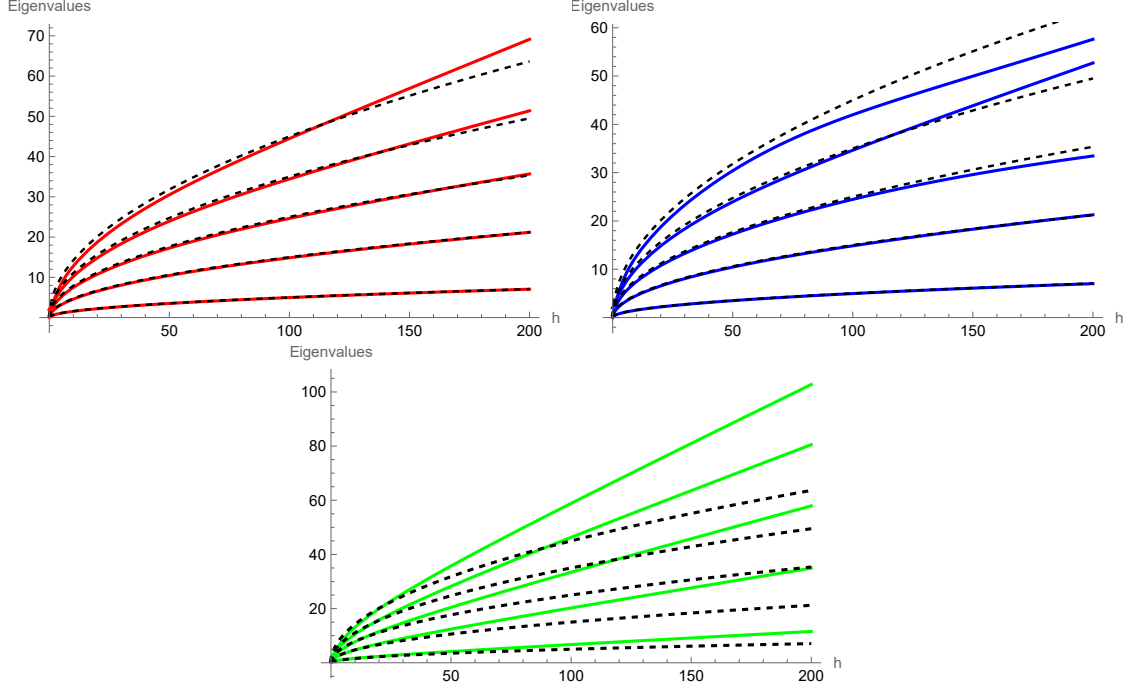


Figure 4: The comparisons of the lowest five eigenvalues of the single link Hamiltonian computed with a small flux cutoff (top left, red curves, $L = 10$), those computed with the discrete Z_N group or a clock model (top right, blue curves, $N = 21$), those computed with the spin truncation (bottom, green curves, $M = 20$), and those of the quantum harmonic oscillator (black dotted curves).

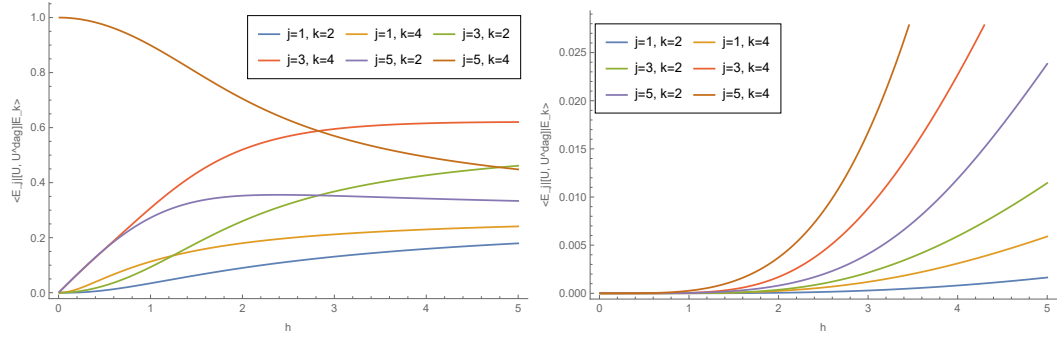


Figure 5: The non-zero matrix elements in the eigenbasis as the functions of h for low spectrum of Eq. (59) with the cutoff $L = 2$ (left) and $L = 4$ (right).

6 Applications to 1 + 1 Field Theories.

We can think of simple 1 + 1-D models to which our scheme can be applied for their simulations. An interesting choice is the Sine-Gordon Model with the Lagrangian

$$\mathcal{L}_{SG} = \frac{1}{2} \partial_\mu \phi \partial_\mu \phi + \frac{m^2}{\beta^2} (1 - \cos(\beta \phi)) \quad (60)$$

This is an intriguing exactly integrable theory with a strong-weak S-duality to the massive Thirring model as shown by [22] by bosonizing the fermion fields of the massive Thirring model, whose fermionic excitations correspond to the solitons in the Sine-Gordon model. We note that the simulation of the massive Thirring model on a quantum circuit is studied in [23]. Both forms could be formulated for qubits with complimentary regions and the challenge to find a common parameter space exhibiting the duality.

Given that the latticized derivative $\partial_\mu \phi := (\phi(x + \mu) - \phi(x))/a$ is small in the low-energy range where a is the lattice spacing, we can express the Sine-Gordon model on the 1 + 1-D lattice in our notation with the mapping of the conjugate momentum field $\pi(x) = \partial_0 \phi(x) \rightarrow E_x$ and the compactified field $\exp(i\beta \phi(x)) \rightarrow U_x$ as

$$\hat{H}_{SG} = \frac{1}{2} \sum_x [E_x^2 + h(2 - U_x - U_x^\dagger)] + J \sum_{\langle x,y \rangle} (2 - U_x U_y^\dagger - U_y U_x^\dagger) \quad (61)$$

where $h = m^2/\beta^2$ and $J = 1/2a^2\beta^2$. We fix the lattice spacing to be $a = 1$ from now. We note that for $h = 0$ this is the classical XY model or the generalized spin XXZ chain with $\Delta = 0$ which has been numerically studied in more detail by Zhang, Meurice and Tsai [12] with tensor networks and the range of truncation of $L = 1, 2, 3, 4$. Among the interesting observations, while all preserve the gapless phase, the model has an infinite-order Gaussian transition for $L = 1$ and only for $L \geq 2$ has a BKT transition. This is a nice example of how physics can depend crucially on the number of qubits. It has been known that the Sine-Gordon model effectively describes the vortices in the XY model with β corresponding to the inverse temperature in the XY model, and on the Sine-Gordon side, its BKT transition is well-studied from its renormalization flow [24].

6.1 Real-time evolution

It is plausible that for the small M qubit formulation, we can explore the small h and J region. This indicates that the qubit Hamiltonian is expected to be the effective theory of the exact Hamiltonian in the low-temperature limit. Here, we give the simplest approximation $L = 1$, and simulate the real-time evolution of a state under the Hamiltonian with quantum circuits defined on six lattice sites. For $L = 1$, the Hamiltonian \hat{H}_{SG} can be represented with sigma matrices on a $1 + 1$ -D lattice (ignoring the constant) as

$$H_{SG} = \frac{1}{8} \sum_x \sigma_{x,1}^3 \sigma_{x,2}^3 - \frac{h}{2\sqrt{2}} \sum_x (\sigma_{x,1}^1 + \sigma_{x,2}^1) - \frac{J}{2} \sum_{\langle x,y \rangle} \sum_{i,j=1}^2 (\sigma_{x,i}^+ \sigma_{y,j}^- + \sigma_{x,j}^- \sigma_{y,i}^+) \quad (62)$$

Since the first electric term, the second potential term, and the third interaction term of H_{SG} do not commute with each other, we use the Trotter-Suzuki approximation to simulate the time-evolution operator $e^{-iH_{SG}t}$ on a quantum circuit:

$$e^{-itH_{SG}} \approx \left(\prod_x e^{-i(t/n)(1/8)\sigma_{x,1}^3 \sigma_{x,2}^3} \prod_x e^{i(t/n)(h/2\sqrt{2})(\sigma_{x,1}^1 + \sigma_{x,2}^1)} \prod_{\langle x,y \rangle} \prod_{i,j=1}^2 e^{i(t/n)(J/2)(\sigma_{x,i}^+ \sigma_{y,j}^- + \sigma_{x,j}^- \sigma_{y,i}^+)} \right)^n \quad (63)$$

where $n \gg 1 \Rightarrow t/n \ll 1$. We call the product inside the bracket a Trotter step, and a single Trotter step can be realized as Fig. 6. Each unitary rotation component can be realized with a simple one or two-qubit quantum circuits. Eq. (63) means that we can approximate the time evolution $e^{-itH_{SG}}$ by iterating the Trotter step many times with a small time step of t/n . To test the reliability of the approximated time-evolution operator on a quantum circuit, we construct and simulate the circuit using *qiskit* with six lattice sites, i.e. twelve qubits. We pick the two-point correlation function in the space dimension (specifically, the left-most lattice site and the middle point) as the physical quantity to be measured from the circuit:

$$\langle \cos(\phi(x) - \phi(y)) \rangle \approx \left\langle \frac{U_x^\dagger U_y + U_x U_y^\dagger}{2} \right\rangle = \frac{1}{4} \sum_{\alpha, \beta=1} \langle \sigma_{x,\alpha}^1 \sigma_{y,\beta}^1 + \sigma_{x,\alpha}^2 \sigma_{y,\beta}^2 \rangle \quad (64)$$

Since the observable $U_x^\dagger U_y + U_x U_y^\dagger$ can be expressed as a sum of the product of two sigma matrices with our construction, it can be measured by simple two-qubit measurements on a quantum circuit. We measure each two-qubit Paulis with 4096 runs

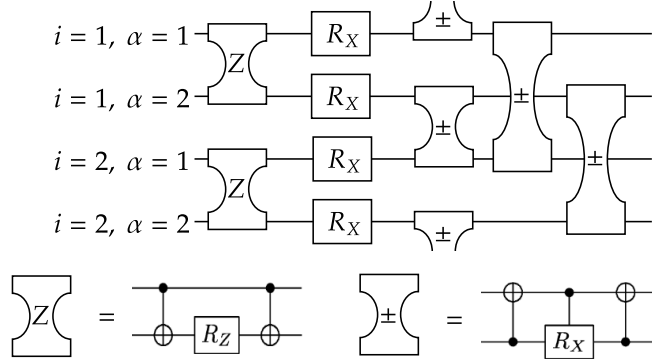


Figure 6: The quantum circuit of the single Trotter step for the Sine-Gordon model for two lattice links with the periodic boundary conditions (top). The index i represents the position of the link and α represents the flavor. The circuit components Z and \pm represent the operator $e^{-i\theta\sigma_{x,1}^3\sigma_{x,2}^3}$ (bottom left) and $e^{-i\theta(\sigma_{x,i}^+\sigma_{y,j}^-+\sigma_{x,i}^-\sigma_{y,j}^+)}$ (bottom right), respectively.

of the circuit to approximate the expectation value. We choose the parameters of the Hamiltonian to be $\hbar = 1$ and $J = 1$, and the state $|\psi\rangle = |00\dots 0\rangle$ corresponding to the state whose links all have the flux of $\ell = -1$ as the initial state which can be easily realized on a quantum circuit. The result of the simulation is Fig. 7, from which we can see that if the value of the time interval t/n is small enough (≈ 0.1), the quantum circuit well approximates the exact time evolution.

6.2 Gapped/gapless phase transition

As we mentioned above, the interesting physical feature to investigate for these $1+1$ -D models in the continuum is the BKT transition. Since the BKT transition is due to the topological defects in the model, for example, the transition in the 2-D classical XY model can be explained as the confinement/deconfinement phase transition of the vortex-antivortex pairs, it is regarded as a topological phase transition. The topologically ordered phase is gapped, i.e. has a finite correlation length ξ . The topological phase transition closes this mass gap and allows the system to have mass-

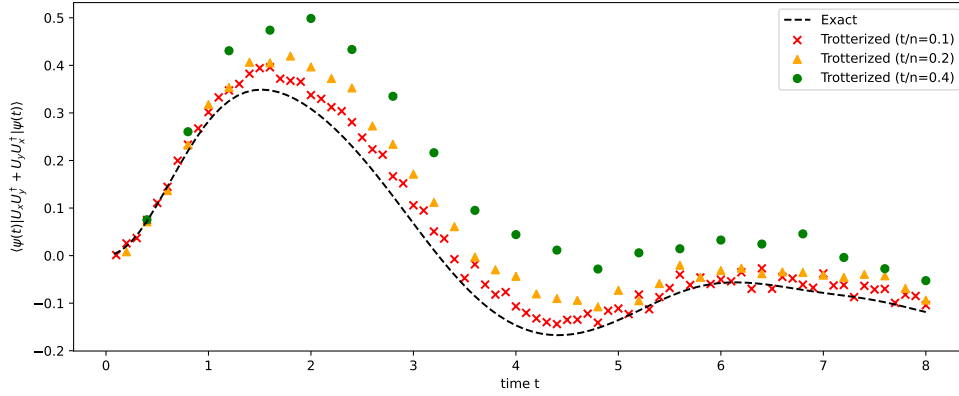


Figure 7: The simulated time evolution of the value $\left\langle \frac{U_x^\dagger U_y + U_x U_y^\dagger}{2} \right\rangle$ with $|\psi\rangle = |00\dots 000\rangle$ with different time intervals ($t/n = 0.1, 0.2, 0.4$).

less Nambu-Goldstone excitations, and hence this other phase is gapless and has an infinite correlation length.

We can observe this gapped/gapless transition by computing the entanglement entropy (EE) of the ground state. The von Neumann EE of the ground state for the subsystem A is defined as $S_A := -\text{Tr}[\rho_A \log \rho_A]$ where ρ_A is the density matrix of the ground state in the subsystem A defined as $\rho_A = \text{Tr}_{A^c}[\rho]$ with the density matrix of the ground state ρ in the total system $A \cup A^c$. The α -Renyi entropy is defined as $S_A^{(\alpha)} = \frac{1}{1-\alpha} \log \text{Tr}[\rho_A^\alpha]$, and it is related to the von Neumann EE by $\lim_{\alpha \rightarrow 1} S_A^{(\alpha)} = S_A$ (so-called the *replica trick*). It is proven by Hasting [25] that the EE of the ground state of one-dimensional gapped systems obeys the area law, i.e. it is bounded from above by a constant which is independent of the subsystem size n as

$$S_A \leq S_{\max} = c_0 \xi \log(6\xi) \log(d) 2^{6\xi \log(d)} \quad (65)$$

where d is the dimension of the Hilbert space for each lattice site. On the other hand, the entanglement S_A needs a logarithmic correction $\log(n)$ in a gapless phase or a critical point in the thermodynamic limit, specifically it is proven for one-dimensional systems by Calabrese and Cardy [26] by means of conformal fields theory (CFT). For the finite volume cases, they prove that the Renyi entropy for the 1 + 1-D quantum

system with conformal symmetry on the finite lattice is (ignoring the constant term)

$$S_A^{(\alpha)} = -\frac{\alpha+1}{\alpha} \frac{c}{6} \log\left(\frac{N}{\pi a} \sin\left(\frac{\pi\alpha}{N}\right)\right) \quad (66)$$

which converges to the von Neumann EE in $\alpha \rightarrow \infty$ as

$$S_A = \frac{c}{3} \log\left(\frac{N}{\pi a} \sin\left(\frac{\pi n}{N}\right)\right) \quad (67)$$

In the thermodynamic limit $N \rightarrow \infty$, converges to the logarithmic correction of $\log(n/a)$. c is the central charge which is a particular coefficient specific to each class of the CFTs and appears in the operator product expansions of two stress-energy tensors of the theory.

Zhang [27] computes the von Neumann EE of the ground state of the Hamiltonian Eq. (61) with $h = 0$ and open boundary conditions, and it is confirmed that the gapped/gapless transition happens with $L = 1$ and the system size of $N = 32, 64, 96, 128$ with the subsystem size $n = N/2$ by means of density matrix renormalization group. As we mentioned, the results from [12, 27] indicate that this model with $L = 1$ has the transition called infinite-order gaussian transition, which is distinguished from the BKT transition but still closes/opens the mass gap. We reproduce this result by computing the von Neumann and 2-Renyi EEs from exact diagonalization of the Hamiltonian with much smaller system size of $N = 10$ and the sub-system size of $n = 2, 3, 4, 5$ as functions of β with two disjoint boundaries (Fig. 8).

That we can observe this gapped/gapless transition with only a small system size of $N = 10$ means that even with the current or near-future digital quantum device consisting of less than a hundred qubits, we may reproduce interesting physical phenomena related to a continuous field theory. Let us note that many efficient quantum algorithms for realizing the ground state on qubits for a given spin Hamiltonian have been proposed such as the variational quantum eigensolver [28], the adiabatic state preparation [29], and imaginary time evolution [30, 31], etc, as well as that one can efficiently evaluate the 2-Renyi EE on a digital quantum device by computing the expectation value $\langle GS | \otimes \langle GS | SWAP_A | GS \rangle \otimes | GS \rangle$ where $|GS\rangle \otimes |GS\rangle$ is the two copies of the ground state and $SWAP_A$ is the operation that swaps the qubits in the subsystem A between those two copies [32]. Such expectation values of a unitary operator can be computed by means of the Hadamard test.

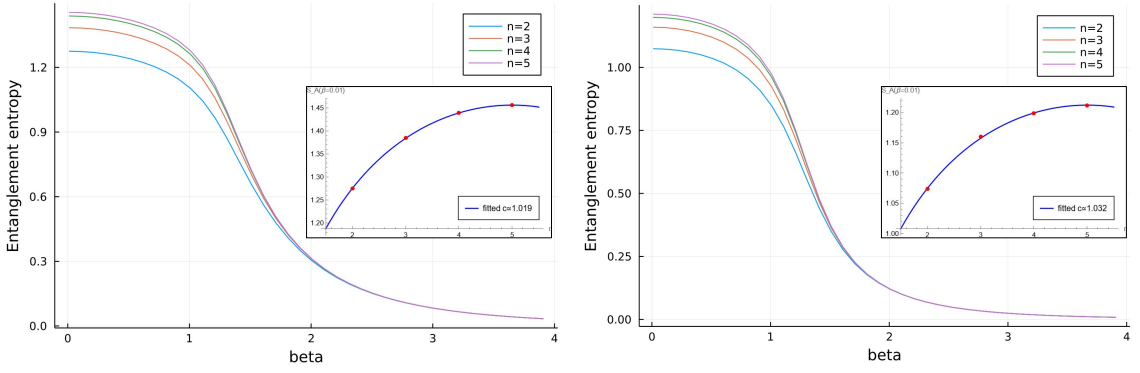


Figure 8: The ground-state von Neumann (left) and Renyi (right) EEs for the system with size of $N = 10$ and the subsystem with size of $n = 2, 3, 4, 5$ with the PBCs. In the small β region, the EEs depends on the subsystem size, and the gaps become smaller as n increases, as we expect for the gapless phase. On the other hand, in the large β region, the EEs become independent of n , so the system must be in the gapped phase. The insets are the values of S_A at $\beta = 0.01$ as functions of the subsystem size n for each boundary conditions (red dots). The value of the central charge c is calculated by fitting the functions Eq. (67) and Eq. (66) (blue curves) as $c \approx 1.019$ for the von Neumann EEs and $c \approx 1.032$ for the 2-Renyi EEs.

We can also find the central charge c of this model by simply linearly fitting the values of S_A and $S_A^{(2)}$ in the gapless phase to the function Eq. (67) and Eq. (66). We fit their values with $\beta = 0.01$, and find that the central charges are $c \approx 1.019$ for S_A and $c \approx 1.032$ for $S_A^{(2)}$, respectively (the insets of Fig. 8). These almost reproduce $c = 1$ which is expected for this class of the model [33, 34].

7 Discussion

In this paper, we have discussed a version of quantum links with *gauged flavor symmetry* [5, 6] focusing especially on the problem of a $U(1)$ quantum link. The main problem we have focused on in this paper is how to realize local degrees of freedom that are effectively bosonic and have a non-trivial symmetry structure realized on them in terms of (fermionic) qubits. Generically, these are ingredients that can be

used on a variety of field theories, not just gauge theories. Such a choice depends if one puts the degrees of freedom on a link or on a lattice site and it would also depend on if one imposes a local symmetry constraint or not, that would involve many links at a time. A single link/lattice variable would not know this on its own. The main problem with bosonic systems is that they naturally have an infinite-dimensional Hilbert space of the states. This needs to be truncated if it is to be simulated on a quantum computer.

The truncation suggested by the fermionic qubits for $U(1)$ picks a particular quantization of a system that has an $SU(2)$ symmetry on phase space, but only a $U(1)$ symmetry in the Hamiltonian. This gives us a quantum theory on a two-sphere, which is realized by angular momentum operators with a fixed value of L^2 . We showed in the classical theory and in the quantum theory how taking $L^2 \rightarrow \infty$ results in the Kogut-Susskind Hamiltonian after an appropriate rescaling of variables. The physics is in a compact phase space locally with finite volume in the units of the quantum \hbar . Taking the volume to infinity can provide the phase space of a tangent bundle on the $U(1)$ manifold if done appropriately. We also showed how additional corrections to the Hamiltonian (which can be thought of as higher derivative corrections) could be added so that the naive flux-truncated Kogut-Susskind Hamiltonian for a single variable could be found exactly, rather than approximately at finite cutoff. This type of argument suggests that the link variables with gauge flavor symmetry fall in the same universality class as Kogut-Susskind type Hamiltonians do in the appropriate limit, without the need to add these higher-order corrections.

Generalizing this construction to other non-Abelian symmetry groups seems to require studying the quantization on a complex Grassmannian (a compact phase space) and taking a similar large volume limit in units of \hbar .

Some special features were found in the $U(1)$ theory where the original problem with $2M$ fermionic qubits could be reduced to M qubits that are effectively hard bosons: they commute with each other. The physics requires that the permutation group between these hard bosons was fully symmetrized between them. The qubit realization of the U, U^\dagger operators resulted in the unique representation that appears from the addition of angular momentum for these variables, with maximal angular momentum.

We studied various versions of the truncated Hamiltonians that differ from each other in the choices that are made for these higher derivative corrections and found good

agreement with the quantum rotor (the Kogut-Susskind Hamiltonian with no cutoff) They supposedly approximate even for moderate values of the coupling. It is interesting to study this property further for other models with non-abelian symmetry.

We also studied other implementations that are not based on the fermionic bilinears, but where the truncation in Hilbert space is done to minimize the number of total qubits, and the embedding is more ad-hoc (there is no natural symmetry action on the qubit degrees of freedom, it needs to be built by hand). At least in this sense, one can talk about the efficiency of the implementation in terms of resources.

We also applied these ideas to the models with two such $U(1)$ degrees of freedom as would appear in a chiral $U(1)$ model on a 1-D lattice. In particular, we showed how a simple truncation could be implemented in terms of explicit gates on a collection of 12-qubits (two per site) and showed how the Trotter expansion could be executed for studying the real-time evolution of a simply prepared initial state. Furthermore, in the $U(1)$ case, we used exact diagonalization to argue that the ground state on a lattice of only 10 sites was already big enough to show non-trivial critical behavior in the entanglement entropy when varying the coupling constant. This suggests that interesting physics at (or near) criticality can be simulated on a modest quantum computer with roughly ~ 100 qubits, rather than requiring us to take the large volume limit first.

What is left out in this study is any serious exploration of how a minimal number of qubit per lattice site might preserve the universality class. Indeed this is a central and very challenging dynamical problem depending on the existence of a second-order critical surface. While preserving the symplectic algebra on the local field is clearly an attractive requirement, it does not address this problem. As in the classical Ising Hamiltonian with a single qubit per site with Z_2 reflection, the collective dynamics across the spatial lattice is sufficient to guarantee universality.

There are many potential routes to universality. For example, we have also left out the original quantum link conjecture that in an asymptotically free theory (non-Abelian 2d sigma model or 4d gauge theory), flavors distributed in an extra dimension are sufficient to guarantee universality. Such models break the flavor symmetry but would also reduce the number of quantum gates to be executed to logarithmic growth in the correlation length. Our previous work [35], for example, provides such an implementation for a $U(1)$ gauge theory in $2 + 1$ dimensions. One needs to worry that the breaking of the flavor symmetry done in the Hamiltonian does not pollute

the infrared physics with new degrees of freedom that are not gapped sufficiently. With full gauging of flavor, as we studied here, there are no additional singlet states beyond those required to match the Hilbert space of interest, so the only question is if we approximated the correct Hamiltonian well enough in the low energy sector. A full treatment of such questions needs to be explored in detail.

Acknowledgements

This work was supported in part by the U.S. Department of Energy (DOE) under Award No. DE-SC0019139 and under DE-SC0015845 for RCB. HK was supported by Yukawa Institute for Theoretical Physics (YITP) for the expenses during the visit in Summer 2021 and would like to thank their hospitality. HK would like to thank Suguru Endo, Masazumi Honda, Thomas Lloyd, and Jin Zhang for fruitful discussions and information.

References

- [1] S. Chandrasekharan and U. J. Wiese. Quantum link models: A Discrete approach to gauge theories. *Nucl. Phys.*, B492:455–474, 1997.
- [2] R. Brower, S. Chandrasekharan, and U. J. Wiese. QCD as a quantum link model. *Phys. Rev.*, D60:094502, 1999.
- [3] B. B. Beard, R. C. Brower, S. Chandrasekharan, D. Chen, A. Tsapalis, and U. J. Wiese. D-theory: Field theory via dimensional reduction of discrete variables. *Nucl. Phys. Proc. Suppl.*, 63:775–789, 1998.
- [4] Uwe-Jens Wiese. From quantum link models to d-theory: A resource efficient framework for the quantum simulation and computation of gauge theories, 2021.
- [5] B. Schlittgen and U. J. Wiese. Low-energy effective theories of quantum spin and quantum link models. *Phys. Rev.*, D63:085007, 2001.

- [6] O. Bar, R. Brower, B. Schlittgen, and U. J. Wiese. Quantum link models with many rishon flavors and with many colors. *Nucl. Phys. Proc. Suppl.*, 106:1019–1024, 2002.
- [7] N. Brambilla et al. QCD and Strongly Coupled Gauge Theories: Challenges and Perspectives. *Eur. Phys. J.*, C74(10):2981, 2014.
- [8] R. Brower, S. Chandrasekharan, S. Riederer, and U. J. Wiese. D theory: Field quantization by dimensional reduction of discrete variables. *Nucl. Phys.*, B693:149–175, 2004.
- [9] Sergey B. Bravyi and Alexei Yu. Kitaev. Fermionic quantum computation. *Annals of Physics*, 298(1):210–226, May 2002.
- [10] Richard P Feynman. Simulating physics with computers. *International journal of theoretical physics*, 21(6):467–488, 1982.
- [11] Tanmoy Bhattacharya, Alexander J. Buser, Shailesh Chandrasekharan, Rajan Gupta, and Hersh Singh. Qubit regularization of asymptotic freedom. *Phys. Rev. Lett.*, 126(17):172001, 2021.
- [12] Jin Zhang, Y. Meurice, and S. W. Tsai. Truncation effects in the charge representation of the O(2) model. *Phys. Rev.*, B103(24):245137, 2021.
- [13] Philippe Raynal, Amir Kalev, Jun Suzuki, and Berthold-Georg Englert. Encoding many qubits in a rotor. *Physical Review A*, 81(5), May 2010.
- [14] Victor V Albert, Saverio Pascazio, and Michel H Devoret. General phase spaces: from discrete variables to rotor and continuum limits. *Journal of Physics A: Mathematical and Theoretical*, 50(50):504002, nov 2017.
- [15] David Berenstein. A Matrix model for a quantum Hall droplet with manifest particle-hole symmetry. *Phys. Rev.*, D71:085001, 2005.
- [16] David Berenstein and Robert de Mello Koch. Gauged fermionic matrix quantum mechanics. *JHEP*, 03:185, 2019.
- [17] David J. Gross and Washington Taylor. Two-dimensional QCD is a string theory. *Nucl. Phys.*, B400:181–208, 1993.
- [18] Michael Creutz, Laurence Jacobs, and Claudio Rebbi. Monte carlo computations in lattice gauge theories. *Physics Reports*, 95(4):201–282, 1983.

- [19] Yasuhiro Takahashi. Quantum arithmetic circuits: A survey. *IEICE Transactions*, 92-A:1276–1283, 05 2009.
- [20] Yasuhiro Takahashi and Noboru Kunihiro. A fast quantum circuit for addition with few qubits. *Quantum Info. Comput.*, 8(6):636–649, jul 2008.
- [21] Andrei V. Smilga. *Lectures on quantum chromodynamics*. WSP, Singapore, 2001.
- [22] Sidney Coleman. Quantum sine-gordon equation as the massive thirring model. *Phys. Rev. D*, 11:2088–2097, Apr 1975.
- [23] Chinmay Mishra, Shane Thompson, Raphael Pooser, and George Siopsis. Quantum Computation of the Massive Thirring Model. 12 2019.
- [24] A. O. Gogolin, A. A. Nersesian, and A. M. Tsvelik. *Bosonization and strongly correlated systems*. 2004.
- [25] M B Hastings. An area law for one-dimensional quantum systems. *Journal of Statistical Mechanics: Theory and Experiment*, 2007(08):P08024–P08024, 8 2007.
- [26] Pasquale Calabrese and John L. Cardy. Entanglement entropy and quantum field theory. *J. Stat. Mech.*, 0406:P06002, 2004.
- [27] Jin Zhang. Fidelity and entanglement entropy for infinite-order phase transitions. 8 2021.
- [28] Alberto Peruzzo, Jarrod McClean, Peter Shadbolt, Man-Hong Yung, Xiao-Qi Zhou, Peter J. Love, Alán Aspuru-Guzik, and Jeremy L. O’Brien. A variational eigenvalue solver on a photonic quantum processor. *Nature Communications*, 5(1), Jul 2014.
- [29] Edward Farhi, Jeffrey Goldstone, Sam Gutmann, and Michael Sipser. Quantum computation by adiabatic evolution. *arXiv preprint quant-ph/0001106*, 2000.
- [30] Sam McArdle, Tyson Jones, Suguru Endo, Ying Li, Simon C. Benjamin, and Xiao Yuan. Variational ansatz-based quantum simulation of imaginary time evolution. *npj Quantum Information*, 5(1), Sep 2019.
- [31] Mario Motta, Chong Sun, Adrian T. K. Tan, Matthew J. O’Rourke, Erika Ye, Austin J. Minnich, Fernando G. S. L. Brandão, and Garnet Kin-Lic Chan. Determining eigenstates and thermal states on a quantum computer using quantum imaginary time evolution. *Nature Physics*, 16(2):205–210, Nov 2019.

- [32] Matthew B. Hastings, Iván González, Ann B. Kallin, and Roger G. Melko. Measuring Renyi Entanglement Entropy in Quantum Monte Carlo Simulations. *Phys. Rev. Lett.*, 104(15):157201, 2010.
- [33] C R Allton and C J Hamer. The (1+1)do(2) model: a finite lattice analysis. *Journal of Physics A: Mathematical and General*, 21(10):2417–2429, may 1988.
- [34] Philippe Di Francesco, Pierre Mathieu, and David Sénéchal. *Conformal Field Theory*. Springer New York, New York, NY, 1997.
- [35] Richard C. Brower, David Berenstein, and Hiroki Kawai. Lattice Gauge Theory for a Quantum Computer. *PoS*, LATTICE2019:112, 2020.